Institute FOR Transuranium Elements

JOINT RESEARCH CENTRE

COMMISSION OF THE EUROPEAN COMMUNITIES

EUR 12849 EN

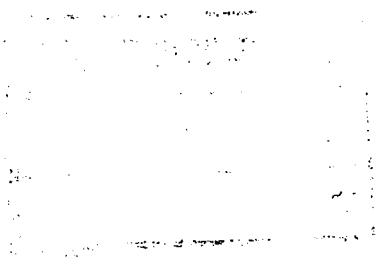

COMMISSION OF THE EUROPEAN COMMUNITIES

Joint Research Centre

INSTITUTE
FOR TRANSURANIUM ELEMENTS
KARLSRUHE

Annual Report 1989

TUAR-89

1990

EUR 12849 EN

Published by the
COMMISSION OF THE EUROPEAN COMMUNITIES
Directorate-General
Telecommunications, Information Industries and Innovation
Bâtiment Jean Monnet
LUXEMBOURG

Luxembourg: Office for Official Publications of the European Communities, 1990

Catalogue nummer: CD-NA-12849-EN-C

ECSC-EEC-EAEC, Brussels Luxembourg, 1990

Printed in the Federal Republic of Germany

Abstract

In view of an increasing demand for knowledge on fuel performance under high burn-up conditions, *Basic Safety Research on Nuclear Fuels* was concentrated in 1989 on the study of novel fuel concepts: Transient-tested high burn-up fuel samples were investigated by electron microscopy to study the effect of strain on fission product distribution, and the concentration of $(U,Pu)O_2$ agglomerates in irradiated MOX fuel was examined by electron microprobe analysis.

Conclusions on maximum temperatures to which the core of the Three Mile Island reactor was exposed could be drawn from an examination of TMI fuel debris.

Equipment to measure thermophysical fuel properties such as thermal conductivity, specific heat, thermal expansion and optical emissivity at temperatures of interest for reactor safety studies was further developed.

An improved version ("slice version") of the TRANSURANUS fuel pin code was tested and released for external use.

Safety Aspects of Fuel Operation and Handling were dealt with by improving preparation methods for uranium-plutonium mixed nitride and investigating the behaviour of (U,Pu)N of different origin in the fast flux of the French PHENIX reactor.

Release and resuspension of radioactive dust particles in fires was studied, both in large-scale simulation experiments and with mixed oxide fuel samples in a glove box.

The principal objective of the *Actinide Determination and Recycling* activity was the reduction of long-term hazards of alpha-bearing nuclear waste. In this context, the behaviour of minor actinide oxide fuel in a fast reactor was investigated, and the risk factor reduction obtained by coupling light water reactors and fast reactors was evaluated.

The long-term storage behaviour of UO_2 and MOX spent fuel samples as well as of vitrified waste forms was further investigated within the frame of an activity on the *Characterisation of Waste Forms and High Burn-Up Fuel* by studying the effect of leaching in various environments.

The elucidation of the electronic structure of the transuranium elements is the central objective of basic *Actinide Research* at the Institute for Transuranium Elements. A large number of ternary alloys containing Np or Pu and Si or Ge, together with a transition metal as the third component, was prepared for basic experimental studies. The cohesive properties of lawrencium were calculated from first principles. New high-pressure phases were discovered in PuSe, UPS, ThO_2, and PuO_2.

Exploratory Research concerned the relationship between sound pressure level and the agglomeration rate of aerosol particles subject to a high-intensity acoustic field.

The Institute gave, as in the past *Scientific-Technical Support to Community Policies* by performing analytical work on behalf of the EURATOM Safeguards Directorate. In the same context, analytical techniques were evaluated and automated for the safeguards Service of the International Atomic Energy Agency. A multiwavelength pyrometer was adapted for industrial use upon request of the Commission`s Innovation and Technological Transfer Directorate.

Major contracts with Third Parties under execution or negociation were dealing with the development of minor actinide alloys, the preparation of alpha-emitting nuclides for radio-pharmaceutical purposes, and the post-irradiation examination of high burn-up UO_2 and MOX fuel from LWR power stations.

Table of Contents

Foreword

to the Annual Progress Report 1989
of the European Institute for Transuranium Elements
(TUAR 89)

Since 1987, reporting on progress of work performed at the Institute for Transuranium Elements (ITU) is done in an annual sequence, and previous semestrial reports (TUSR) have been replaced by annual reports (TUAR). Moreover, former semestrial reports were dealing exclusively with studies concerning the JRC programme on Nuclear Fuels and Actinide Research, while the TUARs have become Institute's reports, covering all fields of research treated at the Institute.

Whereas TUAR 87 and TUAR 88 were organized along the JRC programme scheme, an attempt is made to present the "Main Achievements" of the specific programme work executed at the ITU in 1989 in a sequence of five chapters, thus reflecting the internal structure of the Institute which is organized in five scientific/technical Special Services. This presentation simplifies the preparation, facilitates the reading of the report, and avoids unnecessary repetitions.

The reduction in volume (as compared to previous Institute's reports) is the consequence of an attempt to homogenize the reports from all nine JRC Institutes. They will also have an identical new cover.

Also in 1989, the staff of the Institute for Transuranium Elements was very productive, as this is demonstrated by the list of publications in the annex of this report, inspite of the obligation to perform an increasing amount of contract work for external partners from industry and national institutions.

J. van Geel
Director

Karlsruhe, April 1990

Executive Summary

Introduction

Nuclear Safety was, as in the preceding years, the principal theme of the work of the Institute for Transuranium Elements in 1989. Research and development work deals with

- efforts to improve the safety of nuclear fuel operation under normal working conditions, in the presence of power transients, and in accident situations,

- safety aspects of fuel handling, and here in particular the study of release mechanisms and possibilities of retention and scavenging of nuclear aerosols,

- actinide determination in spent fuel and an investigation of the possibilities and consequences of actinide recycling in power reactors,

- the characterisation of nuclear waste forms (simulated and real vitrified waste and spent fuel) and preparations for high burn-up fuel chemistry studies, and

- basic actinide research.

The majority of these studies are performed in the frame of the specific JRC programme on Nuclear Fuels and Actinide Research, while certain activities in the field of fuel safety were initiated by the JRC programme on Reactor Safety and the studies on nuclear waste characterisation are part of the JRC Nuclear Waste Management Programme. Work on acoustic aerosol scavenging is in an exploratory stage.

In addition, the Institute has continued its support of Community policies in the field of nuclear safeguards by performing safeguards analyses for the EURATOM Safeguards Directorate and by developing and improving radio-analytical techniques in collaboration with the International Atomic Energy Agency. Very recently the Institute became involved in a collaboration with the Commission Innovation and Technology Transfer Directorate aiming at the transformation of a prototype high-speed pyrometer developed at the Institute into a product apt for industrial applications.

Work against payment from third parties involved about 4% of the Institute's research capacity in 1989.

The total Commission staff (not including scientific visitors, student trainees, doctoral fellows and local temporary agents) evolved from 186 at the beginning of the year to 197 by the end of 1989.

Specific Programmes

Basic Safety Research on Nuclear Fuels

A comprehensive investigation is being performed at the Institute on processes and mechanisms occurring in LWR fuels up to very high burn-ups (i.e. 60 GWd/t). For this purpose, well planned laboratory experiments to provide basic fuel data are complemented with the results of specially designed irradiation experiments, and the combined results are then used to develop and validate computer codes which should predict the fuel behaviour over a wide range of operation conditions (normal, transient, and accidental).

In 1989, fuel samples which had been base-irradiated to about 4.5% burn-up and then transient tested to around 41 kW/m in the frame of an international cooperation (International Fission Gas Release Project Risø III) were subject to electron microscopic and electron microprobe analysis (an important achievement, which rarely has been attempted before!). The same type of examination was applied to irradiated LWR fuel pins containing small amounts of plutonium (MOX fuel).

In view of the increasing importance of MOX (UO_2 with additions of PuO_2) as light water reactor fuel, MOX fuel samples which had been irradiated to 39 GWd/t have been examined by electron microprobe analysis, and it was found that the concentration of MOX agglomerates decreased with increasing distance from the fuel pin center.

Laboratory studies on simulated high burn-up fuel (SIMFUEL) gave evidence for a very small effect of the presence of fission products on the rare gas mobility, an effect which is much smaller than postulated in the literature. The consequences of this observation are being analysed.

From an examination of samples extracted from the melted-down core of the TMI-2 reactor, evidence was obtained about the mechanisms of the reactor melt down and the core temperature reached during the accident.

The thermal conductivity of molten UO_2 was remeasured (and previous results obtained in this laboratory confirmed). - An apparatus for measuring the specific heat of acoustically levitated fuel samples up to very high temperatures (in the solid and the molten state) was further improved. - The spectral emissivity of UO_2 was measured up to 4000 K and attempts are under way to provide a theoretical basis for the observations.

The TRANSURANUS fuel pin code has been further improved and applied to the interpretation of the Risø III experiments and, in combination with the FUTURE code developed at the Institute, to fission gas release modelling. The latest edition of the FBR version of TRANSURANUS, including the so-called "slice version", was released to the European Accident Code development group at Ispra. It took into account various specific requirements from the EAC team.

Safety Aspects of Fuel Operation and Handling

During the period under report, the basic studies on porous uranium-plutonium-nitride with a high thermal stability at a specified material density of 80 to 85% TD were continued. By varying the consolidation procedure, a very promising reaction product was obtained which is being tested between 1875 and 2400 K both under isothermal conditions and in an applied radial temperature gradient.

The irradiation in the PHENIX reactor of mixed nitride fuel pins prepared by different procedures (NIMPHE 1) was completed and the pins are undergoing non-destructive analysis in the hot cells of CEN Cadarache. The irradiation of NIMPHE 2 continues.

The study of the release of - simulated - radioactive aerosols from a glove box fire was continued with the installation of a cascade impactor into the fire test chamber. The results of these studies will contribute to an evaluation of the risk of contamination originating from a fire in a nuclear installation.

The resuspension mechanisms of radioactive dust particles was investigated with uranium-plutonium oxide particles in a glove box. Earlier findings were confirmed, that at most 2% of the inventory of radioactive particles can be expected to be transported to the ventilation ducting of a room in which a glove box fire occurs.

Actinide Determination and Recycling

It could be shown in 1989 that inductively-coupled plasma mass spectrometry (ICP-MS) is an appropriate technique to analyse Np concentrations in the 100 ppb range. The technique has been employed to measure Np concentrations in fuel samples discharged from the KNK IIb experiment,

The fast flux experiment SUPERFACT, determined to study the in-pile behaviour of minor actinide containing fuel and carried out in the PHENIX reactor, is presently awaiting analysis in the Institute's hot cells.

The study of a coupling of light water reactors and fast reactors to the transuranium element fuel cycle has shown that the long-term hazard of α-bearing waste can be reduced by a factor of at least 200 when all transuranium elements are recycled.

Characterisation of Waste Forms and High Burn-Up Fuels

The objective of studies on the characterisation of nuclear waste forms is to investigate the thermal and mechanical stability of unprocessed spent fuels and of high level vitrified waste under conditions of long-term storage. They comprise measurements of the radioactive nuclide inventory, determination of the redistribution of actinides and fission products, performance of leach tests with various leachant compositions and studies of the effects of radiation damage on the long-term storage behaviour of the waste material.

During the period under report, *unirradiated fuel samples* were subjected to leach tests and the surface of these samples was analysed by Rutherford backscattering and channeling techniques. The hydrogen takeup at the surface was measured by elastic recoil detection analysis. The results indicated that at 200°C thick layers of

hydrated UO_3 had formed on the surface of the samples. Similar measurements are being performed on UO_2 fuel samples with simulated burn-up.

Leach tests with *spent UO_2 and MOX fuel specimens* have been conducted by means of Soxhlet extractors over periods of 7, 30 and 100 days. It was found that the platelet-like phase (believed to be U_4O_{9-x}) on the surface of the as-irradiated samples disappeared during leaching and that Cs, Si, Cl, and Ca were released from phases which had formed on the inner side of the cladding. The results of these experiments will help to understand and quantify the various processes affecting the stability of fuel during long-term storage.

Investigations into the long-term storage behaviour of *vitrified waste* by studying the effects of alpha radiation damage in ^{244}Cm doped glasses demonstrated that radiation damage significantly increased the fracture toughness of the glasses, a positive effect, if one considers their technical application. Damage caused by controlled ion implantation at elevated temperatures (up to 450 °C) increased the leach rate of the glasses and caused changes in the sodium distribution. The significance of these findings for the long-term storage behaviour of vitrified waste is being evaluated. This programme herewith comes to an end.

Actinide Research

The central objective of actinide research at the Institute, as well as in its numerous collaborations, is the elucidation of the electronic structure of actinide metals and actinide compounds, in particular of the behaviour of the 5f electrons. The dualism between localized and itinerant characteristics as it is particularly clearly demonstrated in the actinide series, is a key problem in these studies.

These goals are approached by experiment and theory.An important basis for the experimental study is the preparation of polycrystalline and single crystal samples of actinides of high specific activity, and their careful characterisation by x-ray diffraction, chemical, and electron microprobe analysis.

As in previous years, the preparation of chemically pure, single phase, and well characterised compounds of actinides of high specific activity was a basis not only for solid state physics work at the Institute, but also in a wide variety of collaborations with external laboratories. Single crystals were grown from part of these compounds. The accent this year was on ternary compounds of neptunium or plutonium with silicon or germanium, and a transition metal as the third component. Twenty eight of these compounds were prepared and crystallographically characterised for the first time.

Calculations of the cohesive properties from first principles indicate that lawrencium is not a simple sp metal, but the first member of a 6d transition series.

New high-pressure phases were found for PuSe, U(P,S) and the dioxides ThO_2 and PuO_2.

The diagram of phase relations of the lanthanide metals was completed by a high-pressure study of promethium, the only rare earth metal which had not yet been studied under pressure.

Work continued on the complex low-temperature phase transitions in alpha uranium.

A new effort to examine magnetic effects with synchrotron X-ray radiation was initiated this year.

Exploratory Research

The feasibility of the use of high intensity acoustic waves to combat airborne spreading of accidentally released radioactive or toxic material has been investigated for the past two years. During the reporting period the acoustic agglomeration of submicron combustion aerosols produced by burning rubber in a 15 m^3 chamber was studied and compared to earlier results obtained in a 4.5 m^3 chamber. The results have shown that increasing the sound pressure level drastically increases the agglomeration rate, their sedimentation velocity, however, increases only slightly due to the fact that smoke agglomerates are open structures with modest aerodynamic diametres.

Future experiments will concentrate on acoustic agglomeration of well defined aerosols under dynamic flow conditions. A potential application is here the acoustic pretreatment of fine particles in gas streams to increase particles sizes and hence the efficiency of electrostatic filters or cyclones to remove them. The necessary equipment is being installed.

Scientific Technical Support to Commission Services

Analytical Support to the EURATOM Safeguards Directorate (DG XVII)

Part of the continuing support to the European Commission consists of the analysis of Safeguards samples collected and sent by the Nuclear Inspectorate, Luxembourg.

As part of the on-line evaluation of data, an expert system has been further developed and extended to include an automatic titration device during the reporting period.

This apparatus (an automatic titrator, type RADIOMETER) is being connected to the central PDP-11 computer system, and a visual display unit allows the operator to start the programs and to keep an overview, on-line, of the data already collected held in the form of a databank.

The titration requests will be generated by the expert system which causes the bar-code labels for the sample containers (dissolution, dilution, weighing and titration) to be printed and determines the sample and details of the aliquotation for the titrator operator.

Already planned (and software partly written) is the connection of a K-edge apparatus to the central computer.

The second development activity concerns the analysis of solid residues in HAW or input solutions. At present these analyses are being made using destructive techniques but a future method of analysis to be utilised is by inductively coupled plasma/mass spectrometry (ICP-MS) employing the technique of laser ablation directly on the solid material.

The third activity concerns the development of an on-site laboratory to be situated at a processing plant and capable of analysing the input and output of the plant for Safeguards. This work is at the stage that a conceptual report is being prepared.

The flow of the measurements and the necessary checking will be controlled from the Institute. This will involve not only the statistical supervision of the measured

results but also the initiation of standards which will be inserted into the measurement stream.

Evaluation and Automation of Analytical Techniques (DG I)

Four tasks are currently being carried out in the frame of the EURATOM/IAEA support programme:

- The development of software for quality control of analytical results on input samples. Existing software will be used and re-written to include the quality control feature.

- The rationalisation of analytical work, particularly in respect to reprocessing plant samples. This activity deals essentially with the field-testing of a K-edge apparatus.

- The automatic conditioning of samples by robots. Here, the instruction manual has been written and will shortly be delivered. A joint evaluation and exchange of experience made with the robot will be made shortly.

- The execution of a cooperative field test of on-site sample conditioning by robots. The IAEA has defined the pilot plant at Gatchina near Leningrad as a site where the testing can be carried out. The scope of the experiment and the design of the robot are at present under discussion.

Adaptation of a rapid multiwavelength pyrometer to industrial use (DGXIII)

An optical instrument for precisely measuring temperatures at very short intervals (milliseconds) and independent of the emissivity of the source has been developed at our laboratories and will be adapted to use in an industrial environment with the support of the Innovation and Technological Transfer Directorate of the Commission.

Work for Third Parties

The Institute continued its support of other JRC Laboratories by fabricating, for example, plutonium dioxide sol-gel spheres for the DARM project. In addition the ITU had in 1989 about 20 contracts with third parties under study. In several cases, however, efforts had to be limited to preparatory work, if the investigation on radioactive material, in particular irradiated fuel specimens from outside partners were involved, due to transportation problems beyond our control.

Activities for third parties concerned

- the execution of boron analysis on samples from nuclear power stations,
- the purification and storage of enriched UO_2,
- Plutonium determinations and the chemical analysis of MOX fuel,
- a design study for a robotized radio-analytical laboratory,

- the preparation and characterisation of alloys containing the "minor" actinides (Np, Am, and Cm),

  and

- the preparation of alpha-emitters for radiotherapeutical applications.

Major contracts dealing with the analysis of reprocessing residues and with the post-irradiation examination of LWR fuel rods are under preparation.

The total volume of all contracts under study and under preparation (some of them extending over several years) is of the order of 3 million ECU.

Presently, somewhat more than 3% of the Institute´s S/T-staff is involved in third-party work.

Associated Laboratories

The Institute is closely collaborating with an international group of laboratories in the Risø fission gas release study project, where the fuel structures of and the fission gas release mechanisms acting in high burn-up light water reactor fuel subjected to ramp tests is studied in a cooperative effort.

Several tasks related to the international PHEBUS PF project (development of in-pile temperature measuring devices and fission product release studies) have been or will be assigned to the Institute.

In the field of basic actinide research, the Institute maintains its central role on the international research scene. In 1989, 32 European and 8 US laboratories have actively collaborated with the Transuranium Institute. In most cases, samples (mostly single crystals) of actinides and actinide compounds produced in our laboratories have been subjected to solid-state investigations in outside laboratories (synchrotron radiation facilities, neutron diffraction equipment, magnetic properties measuring apparatus), and the results thus obtained were analysed (and in most cases published) in a joint effort by ITU and external staff.

1.Main Achievements and Milestones

1.1 Specific Programmes

1.1.1 Basic Safety Research on Nuclear Fuels

With the aim to improve the safety of nuclear fuels, a comprehensive investigation is being performed at the Institute on processes and mechanisms occurring in LWR oxide fuels up to very high burn-ups (~ 60 GWd/t U), which are of relevance for the fuel behaviour under both operating transient conditions and in accident situations. The underlying philosophy, practized at ITU for many years, is to perform well planned laboratory experiments providing basic fuel data in parallel with the careful post-irradiation analysis of fuel which has been irradiated under steady state, transient or accident conditions up to high burn-up , and to use the results thus obtained to develop and validate computer codes which then should be able to predict the fuel behaviour over a wide range of conditions. The actions taken in this context comprise

- so-called *"single effect studies"* whereby the release of selectively introduced interesting fission products like iodine (e.g. by ion implantation) into UO_2 with different simulated burn-ups is measured under well controlled conditions,
- hot cell anneals to investigate gas release up to the melting point from UO_2 irradiated to high burn-up,
- the determination of important physical properties (like thermal conductivity and heat capacity) of liquid UO_2,
- a careful post-irradiation examination of debris from the Three Mile Island Reactor,
- cooperation in the Internal Fission Gas Release Study Project Phebus FP, and
- contributions to the development of a European Accident Code for fast breeder reactors.

Structural Investigations and Basic Studies on Fuels, Oxide Fuel Transients

Irradiation Experiment BUMMEL (BUbble Mobility MEasurement Level)

The aim of this experiment is to measure the mobility of fission gas bubbles in UO_2 under realistic in-pile conditions. The first phase of the experiment - the steady state irradiation at 700 °C to produce fission products within the UO_2 lattice - was terminated after 105 irradiation days at a power of 40 W/g leading to a burn-up of 4200 MWd/t.

The two pins were discharged and the second phase was carried out, i.e. an anneal at 1300 °C for 3 h in order to precipitate volatile fission products into bubbles. One

pin will be used to measure bubble sizes and concentrations before applying a temperature gradient to produce a biased bubble mobility. For this pin, the irradiation experiment is terminated.

The third phase - in-pile annealing under a temperature gradient - took place on July 13, 1989. The axial gradient, 1005 °C to 1750 °C along the pin for 2 h corresponded to the specifications. The experiment was therefore successfully terminated.

Structural Investigation of Transient-Tested Fuel

The Cooperation with the International Fission Gas Release Project Risø III was continued in 1989. Specimens of 14 tests, partly provided with central thermocouples to measure the temperatures during the transient testing, were delivered to the Institute and are being carefully analysed. These studies will be brought to an end by 1990.

Studies on Risø fuel in 1989 concerned essentially two pins which had been subject to very high burn-ups (4.56 a/o and 4.66 a/o, respectively), and exposed to final power levels of 42.0 kW/m and 41.5 kW/m during transients.

Both pins were, as in preceding cases, transient tested after prolonged preirradiation. One of them (CB6) has been tested as-delivered, whereas the second one (CB8)had been opened and a central thermocouple introduced prior to the test phase.

Since there were practically no microstructural data on fuels with these high burn-ups available, a series of investigations was carried out applying optical microscopy, electron microprobe analysis (EMPA), transmission electron microscopy (TEM), and scanning electron microscopy (SEM) to study changes in local structure and composition caused by the particular irradiation conditions.

Transmission Electron Microscopy (TEM) has been successfully performed on two peripheral samples and one central sample of the Risø III fission gas release project.

Specimens were prepared for TEM by extracting a small piece from a known radial position on the cross section, and crushing this in ethanol suspension. Drops of the suspension were allowed to dry on carbon support films which were then examined by TEM. This method has the advantages over electropolishing that solid fission product precipitates are not lost and that the sample activity is low, facilitating handling and energy dispersive X-ray analysis. The positional accuracy, however, is not so good as with electropolished samples, and there is the possibility of introducing mechanical damage into the specimens during preparation.

The specimens were examined in the Hitachi H700 HST operating at an accelerating voltage of 200 kV. Energy dispersive X-ray analysis was performed with the Tracor Northern TN5500 system attached to this microscope.

Both samples from the periphery showed similar microstructural changes compared with base irradiated fuel, for CB6 the changes were more pronounced, consistent with the high linear power level reached during the transient. The main microstructural development was the growth of a population of large fission gas bubbles (>30 nm) on the dislocation networks, each bubble usually associated with a solid fission product precipitate. The density of the large fission gas bubbles was around 5×10^{14} cm^{-3}, and the dislocation density 2×10^{10} cm·cm^{-3}, rising to

local values as high as 5 x 10^{11} cm·cm^{-3} in the direct neighbourhood of large solid precipitates.

It was possible to analyse directly some of the large (>100 nm) solid fission product precipitates which had become detached from the matrix during the preparation using energy dispersive X-ray analysis. Mo, Tc and Ru were identified as constituents. These precipitates were always spherical, and electron diffraction showed that they were crystalline, although the structure has not yet been identified.

A very high density of small fission gas bubbles (<5 nm) with a fairly homogeneous distribution and mean density of 1.2 x 10^{16} cm^{-3} was found in both specimens. The population of small fission gas bubbles showed a strong interaction with precipitates of about the same size.

Replica Electron Microscopy was performed on one fuel section of the CB8 pin and on two sections of CB6. The preparation of these replicas was repeated several times and the replicas themselves checked by scanning electron microscopy, because the expected intragranular fission gas bubble development was not seen.

It is now clear from this analysis and from the TEM observations that the intragranular bubble population remains mostly below the 50 nm diameter resolution limit of the REM technique. The replicas show a clear development of the intergranular bubble population in CB6 and CB8, the former development being more advanced as a function of radius than the latter.

Scanning Electron Microscopy (SEM) was performed along a full radius on each of the above fuel cross sections, using the JEOL JEM 35 SEM mounted in a hot cell. Where transgranular fracture had occurred the SEM micrographs confirmed the absence of intragranular fission gas bubbles larger than about 50 nm in diameter.

The radial distribution of retained Xe and Cs has been determined by *Electron Microprobe Analysis (EMPA)* in two sections of the above transient tested LWR fuel. The Xe and Cs retention profiles were typical for fuel subject to high heat loads. There was no release in the cold outer region of the fuel; a sharp drop in concentration occurred at intermediate radial positions, and there was almost total release of Xe and Cs in the central region of the fuel. Between 40 and 50 % of the Xe inventory had been released during the transient compared with 25-40 % of the Cs present. The EMPA profile for Xe matches that obtained by XRF at Risø which suggests that gas retention on the grain boundaries was negligible.

The radial distribution of Ba in the fuel was determined using EMPA and microgamma scanning. In addition, the axial distribution of Ba in the rods was deduced from ^{140}La gamma scans from which the power profile at the transient terminal level was determined. The results show that appreciable redistribution of Ba can take place in high burn-up UO_2 fuel under transient conditions at terminal powers above 38.5 kWm^{-1}. Radial and axial migration occur by vapour transport. Ba-SiO_3 inclusions were observed at intermediate radial positions. These had formed either as the result of condensation of Ba from the hotter central regions of the pellet or as the result of the agglomeration of pre-existing submicroscopic precipitates. In the centre of the fuel, Ba oxide, possibly BaO or $BaZrO_3$ may form.

Although substantial redistribution of Ba had taken place in the transient tests, little Ba had been released to the pin free volume. At the highest power level seen in the Risø transient tests the percentage release did not exceed 5 % of the Ba inventory. Nevertheless, it is concluded from the findings that the percentage of Ba released under transient conditions will depend on the fuel characteristics. Fuel with a low density and a high percentage of open porosity will have a tendency to

release a higher percentage of Ba. On the other hand, fuel with a high impurity level, particularly a high concentration of Si, may show less Ba release due to the formation of ternary oxides.

Microprobe Analysis of MOX Fuel

Uranium dioxide enriched with several percent of PuO_2 (MOX fuel) is more and more used to fuel industrial light water reactors. During the fabrication process, agglomerates enriched in plutonia may form in the fuel matrix. Possible effects of the presence of these inhomogeneities on the irradiation and dissolution behaviour of MOX fuel are of high technical relevance.

The objectives of our current work on MOX agglomerates are fourfold: 1) To determine the effect of agglomerate size on the level of Xe and Cs release. 2) To establish whether the level of Xe and Cs release is different parallel and normal to the radial temperature gradient in the fuel. 3) To see how the composition of the metallic fission product inclusions, particularly the concentration of Mo, changes along the fuel radius. 4) To obtain the local burn-up value in the agglomerates.

For this purpose, a section of MOX Fuel which had been irradiated in a power reactor to a burn-up of 38.8 GWd/tU is being examined by EMPA. Point and area analysis has been used to investigate the radial distribution of Xe, Cs, Pu, Zr and Nd in the matrix. The first results show that the retention profiles for Xe and Cs do not differ significantly from those observed in UO_2 fuel. Pu in the matrix increased with decreasing distance from the fuel centre due to the dissolution of the MOX agglomerates. The fission products Zr and Nd , which are immobile, were found in the UO_2 in appreciable amounts indicating that the burn-up in this material was not negligible. The work will be continued.

Basic Release Laboratory Studies on SIMFUEL

The *basic work* on release of volatile fission products from simulated high burn-up UO_2, called SIMFUEL, was extended to UO_2 with 6 % burn-up. Following a very careful structural examination of the material which proved its merits to act as a simulant for high temperature high burn-up fuel, Kr-85 was introduced by controlled ion implantation. The release of Kr-85 was measured isochronally up to 1500 °C, and isothermally at 1400 and 1500 °C. Different gas concentrations corresponding to release either with or without formation of intragranular bubbles were used, and either a reducing (Ar/8 % H_2) or an oxidizing atmosphere (CO/CO_2) was chosen for the anneals. The results show that the presence of solid fission products has a very small effect on rare gas mobility. The small effect found is an *increase* in the effective diffusion coefficient by at the most a factor of 4 compared with UO_2 without fission products. This is much less than effects postulated in the literature and based on *calculated* temperatures. In contrast, release was very much accelerated for oxidizing conditions. This has been known before for gas concentrations corresponding to low burn-ups. It has now been demonstrated to exist also under conditions of formation of high concentrations of intragranular gas bubbles.

Examination of Samples from the Reactor Core of TMI-2

The Institute has participated since mid-1987, via the OECD, in a programme sponsored by the U.S. Department of Energy to investigate samples extracted from the melted-down core of the TMI-2 reactor. Samples have been drawn from (i) the completely-molten inner core, (ii) the surrounding crust, (iii) the small particle

debris above the upper crust, and (iv) fuel rod remnants from the edge of the reactor pile.

These specimens display the whole range of thermal histories and degradations. The outer edge fuel rod remnants show little sign of overheating and only slight traces of (volatile) fission products on their outer cladding surfaces. By comparison, the molten core specimens revealed a uniform eutectic-type structure of UO_2 and ZrO_2 phases with distributed phases of ferrous (Fe, Cr, Ni) oxides. This structure is derived from the fusion and oxidation of the zircaloy cladding material with the PWR UO_2 fuel; the Ni/Cr/Fe phases result mainly from the melting of the reactor spacer grids and control rod cladding steels (Inconel & 304 s.s. alloys respectively). The small particle debris appeared to contain pieces of UO_2 fuel, degraded/oxidised zircaloy cladding and structural materials.

Our examinations in 1989 have concentrated on the agglomerated crust samples which have shown a very heterogeneous structure with large regions of both ceramic and metallic phases. The metallic phases were principally composed of either Ag (+In) or a two-phase Ni-Fe/Ni-Sn composition. Iron or iron-nickel phases were also seen that were partially oxidised or were in contact with their oxides. The silver inclusions originated from the Ag-15In-5Cd control rod material. The ceramic phases were found to be UO_2 or impure UO_2 with ZrO_2 along with mixed ferrous (Ni, Cr, Fe) and zirconium oxides. The ferrous metal oxides varied in their composition, but pure chromium and iron oxides were observed as well as mixed iron-nickel oxides. This indicates a separation of the elements since the starting material contained all three metals (Inconel: Ni-25Fe-20Cr or 304 stainless steel: Fe-25-Ni-20 Cr).

The above structures give strong clues as to the mechanism of the reactor meltdown and as to the core temperature reached during the accident. The core is believed to have reached about 2500 °C (the eutectic temperature of the Zr (O)-UO_2 system), while the outer crust had a lower and more variable temperature: probably in the region of 1500 °C (i.e. the melting point of stainless steels). One important mechanism for breakdown seems to be the interaction between the stainless steel cladding of the control rods and the zircaloy cladding of the fuel rods to form low-melting metallic and oxide eutectics in the range 1200 - 1400 °C. However, if the silver alloy is released from the control rods then liquid phase dissolution of cladding could be initiated even at its melting point of 800 °C.

High Temperature Properties of Fuels

Work in this field is aimed at assessing basic high temperature properties for the reactor safety analysis. Besides measurements of the thermophysical properties of nuclear fuels at very high temperatures, a new investigation was started covering the migration, release and chemical reactions of radioactive fission products as an effort to enlarge the activities with the twofold purpose of exploiting as much as possible the existing potential and offering to the industry and other research branches advanced and innovative techniques.

Thermophysical Properties

Thermal Conductivity of Liquid Nuclear Fuel: The results of the first measurement campaign which involved the determination of the cross-sectional temperature distribution in a partially molten disc-shaped sample were further analyzed. The possible perturbation effects due to erratic variables or deviations from the

ideal conditions have been evaluated and accounted for. So far the corrections and the residual uncertainties do not invalidate the previous conclusion, i.e. that the thermal conductivity in liquid stoichiometric urania is lower than that at the solidus temperature. (A much debated finding which is in apparent contradiction to earlier findings at Argonne National Laboratory and CEN Fontenay-aux-Roses). Experiments aimed at demonstrating the possible increase of the conductivity in W-doped urania are planned. A positive answer of these tests should definitively clear the discrepancy between our results and those obtained in W-encapsulated urania.

Specific heat of UO_2: Specific heat measurements in a high temperature autoclave are being performed by subjecting an acoustically levitated sphere-shaped sample to a concentric high-power laser flash and measuring the subsequent temperature history at the specimen surface with an ultra-rapid multi wavelength pyrometer. The experimental technique was further improved. The first set of measurements had shown that the spherical samples were subjected to a rather high radial temperature gradient (approximately 500 K/mm). Although the concept underlying the evaluation of C_p is straightforward, the actual procedure of quantifying the relationship between the cooling rate and the specific heat can be quite complicated if the experimental errors are considered. The error analysis was carried out and the significance limits in the different measurements are being established. This investigation is very difficult since the assessment of narrower tolerances often involves implementing non-standard techniques. For instance, in order that C_p can be evaluated with sufficient precision (20%) the error of the cooling rate has to be less than 5 % for cooling rates of the order of one million K/s. This was recently achieved by improving the performance of the six-wavelength pyrometer. New measurements are now in progress with a new experimental setup.

Thermal expansivity measurements: A new high temperature dilatometer has been constructed at the Institute and is now ready for operation. It consists of an X-ray microfocus producing a shadow image of the sample on a special TV tube where an ad-hoc rapid scanning program (patents pending) enables the image to be recorded within one millisecond. After A/D conversion the picture is stored for the evaluation of the expansion coefficient. A computer program has been written to this purpose.

Radiative properties of urania: After the first measurements of the emissivity of urania up to temperatures of 4000 K, a theoretical analysis was untertaken in order to describe the experimental results in terms of a physical model. This will enable the total radiative power to be integrated in the range between 300 and 15000 nm, which covers more than 99 % of the radiated energy at temperatures between 2000 and 7000 K.

Spectral emissivities of refractory metals: Experimental investigations into the high temperature properties of refractory transition metals have rewakened interest in the long standing problem concerning the occurrence of a unique wavelength λ_x to which different emissivity isotherms converge and at which the temperature coefficient vanishes. The existence of such a wavelength, called X-point, has now been confirmed for nine metals. A theoretical explanation of these findings was searched. After the failure of the classical attempt based on the Drude-Zener model, quantum mechanical interband transitions have been assumed to be responsible for the emissivity behaviour near the X-point. A model is proposed which explains the experimental results in terms of merely direct interband transitions, requiring, for consistency, that in the vicinity of λ_x the intraband contributions to the emissivity are vanishing.

New Laser-flash equipment: Instrumentation for the measurement of the thermal diffusivity of irradiated nuclear fuels and highly radioactive nuclear waste glasses in a hot cell has been designed. The laser flash apparatus consists of an HF furnace where a disk shaped sample is heated in a graphite holder whose design minimizes the radial heat transport. A laser pulse is deposited onto one surface of the sample and the resulting temperature variation at the opposite surface is recorded and analyzed to obtain the thermal diffusivity. A special optics is being developed to convey the radiation emitted by the emerging temperature pulse onto a photodetector. Experiments are planned with temperatures down to 600 K using therefore wavelengths in the infrared range from 2000 to 5000 nm .

Thermochemical Properties

Knudsen cell for vaporization of fission products: This apparatus consists of a shielded vaporization cell working up to 3000 K. The fission products released from irradiated nuclear fuels will be analyzed by mass and gamma spectrometry. Heating will take place in vacuo or under (limited) controlled reaction conditions. Work is in progress for the construction of the lead cell and the furnace.

Vapour pressure measurement on mixed nitrides: The furnace was calibrated up to 3250 K and the characterisation of the samples is in progress. A great effort is at present being made to reduce the noise of the mass spectrometer in order to enable the nitrogen peak to be analyzed.

Thermochemistry of fission products: The development of the code MITRA is continuing. The dataset of thermochemical properties collected in a shared-cost action with AERE Harwell and ECN Petten was implemented in our code system for the calculation of the migration and release of radioactive fission products. A computer code for the calculation of the thermochemical equilibrium of about 15 elements and 150 species is being implemented.

Industrial Applications

Construction of a 6-wavelengths pyrometer for industry: Several actions are running aimed at transforming the prototype constructed at the Institute into a compact and reliable product for industrial applications (a patent is pending). Work will be done to increase the sensitivity of the instrument in order to extend the measurement range down to 1500 K. The measuring speed of the instrument was also improved, reaching the sub-millisecond range. Work is also in progress to develop a suitable software for the elaboration of the signals and the calculation of the absolute errors.

Acoustic levitation: With reference to the contacts with industry issued from the presentation of the levitation and splat-cooling device at three international exhibitions, a project for the construction of a levitation furnace was started, in which two major European industries are interested. This will consist of a 20 kHz standing-wave levitator working in an HF-heated susceptor. Temperatures up to 1500 K with various cover gas fillings at moderate pressures should be obtained.

Fuel Pin Modelling with the TRANSURANUS Code

General Code Improvements and Collaborations

TRANSURANUS is a system of computer programmes for the thermal and mechanical analysis of the fuel rods in nuclear reactors. The code is continually being improved. Major effort was given in 1989 to the development of the TRANSURANUS slice version which was necessary for the European Accident Code EAC-2 (see below), to the analysis of Risø-III experiments and to the development of an improved fission gas release model.

The cooperation with other groups using the TRANSURANUS code continued and was expanded. Fuel rod analyses were performed successfully for different fuel rod designs and fuel rod vendors. A good agreement with the results of the vendors was found.

The TRANSURANUS code was successfully installed at an IBM RT PC workstation running under the Aix (Unix) operating system. It has been proved that not only considerable saving in computer cost could be achieved but also significant improvements in the general code development due to the user-friendly Unix environment.

LWR Applications

Interpretation of Risø III experiments: A first attempt at interpretation was performed for the transient experiments II1, II2, III3, AN1, AN2, AN3, AN4, GE2, GE4, which were preirradiated up to $\approx$ 5 a/o burn-up. This interpretation was based on standard TRANSURANUS models. The following results were obtained:

- the assumption that the minimum surface roughness is 5 µm had to be removed, i.e. the gap conductance in the Xe-filled rods is larger than anticipated,
- present models lead to an overprediction of the cladding deformation which is probable caused by an overestimation of gaseous swelling,
- in most cases the measured centre line temperatures were underpredicted,
- as expected, the measured burst release could not be predicted (c.f. improvement of the gas release model below).

A simplified approach to fission gas release modelling: A detailed analysis of fission gas release model for use with the TRANSURANUS code was made. It is suggested that a highly simplified FUTURE version would be more appropriate for inclusion in TRANSURANUS at this stage than the complete FUTURE model. Consequently, a simplified model was developed which consists of the standard expression for intragranular diffusion with simultaneous trapping / re-solution at gas bubbles (Model B). The trapping rate is modified to reproduce in a simple way the "stress field" model for restricted trapping which is the most important feature of the FUTURE model for transient applications. In addition, a semi-empirical model was proposed in which the transient fission gas release is calculated as a function of heating rate and burn-up (Model C). It has been shown that Model B gives an improved agreement with the experimental data and offers an improved calculational route for inclusion in TRANSURANUS. The inclusion of model B will be performed in1990.

Study of the Fuel Behaviour under Accident Conditions using the TRANSURANUS Code

A general revision of the Fast Breeder Reactor version of the TRANSURANUS Code was basically finished and the latest version V1M2J89 was released to the European Accident Code (EAC) development group group at JRC Ispra and to KfK-INR. This version includes the so-called "TRANSURANUS slice version", in which the axial discretisation differs from the standard version: whereas in the standard version an axial fuel pin zone is treated by the analysis at both ends of this axial zone, the analysis in the slice version is done at mid plane position.

Nearly all subroutines were affected by this expansion of the geometrical idealization and therefore all subroutines were not only modified but also generally revised: Structured programming, indentation of loops, if-then-else structures and extensive commenting etc. are now standard to all routines. The revisions and modifications were carefully tested and double-cross checked.

The slice version offers major advantages for use with the EAC-2 code because it avoids very small axial zones at the transition between fertile and fissile zone. Since TRANSURANUS is coupled in the EAC-2 code with fluid - dynamic models which use explicit techniques, the time step in the previous TRANSURANUS version was governed by this small zone due to various Courant conditions. Using the newly developed slice version these small zones could be avoided and a significantly improved performance of the EAC-2 code could be achieved. The slice version was extensively tested against the standard version. It was proved that the predictions of the integral fuel rod behaviour are nearly the same in both versions and differ only due to axial discretisation effects.

Various modifications and improvements of the TRANSURANUS codes were made in response to specific requirements from the EAC group. These improvements together with improvements of the EAC code itself, enabled several whole core accident analyses to be performed successfully with the EAC code.

1.1.2 Safety Aspects of Fuel Operation and Handling

Optimisation of Dense Fuels

Introduction

Mixed nitride (U, Pu)N is considered as an attractive fuel within the frame of the recently reassessed liquid-metal-cooled fast reactor fuel cycle. The possible advantages fo this dense fuel concept has been described before (TUAR 87-88). In order to verify the potential of this concept, a research programme was launched with the aim to compare the performance of nitride, carbide and conventional oxide (U, Pu)O_2 fuel. Within this programme the following stages of the optimised fuel cycle are examined:

- development of fabrication methods and characterisation of the fuel material
- in-pile performance at low (BOL) and high burn-up (> 15 a/o)
- reprocessing of as fabricated and irradiated nitride fuels.

This programme is excecuted in collaboration with the French Commissariat à l'Energie Atomique (CEA), which is responsible for the high burn-up irradiation experiments NIMPHE in the PHENIX reactor and fabricates a part of the nitride test fuel pins.

The contribution of the Institute consists of a more fundamental approach to the fabrication and optimisation of new fuels and fuel pin fabrication for the irradiation experiments NILOC and partially for the irradiation experiments NIMPHE.

Fuel Development

During the reporting period the basic studies on mixed nitrides were continued. The main direction of our investigation was the development of porous nitride fuels with a high thermal stability at a specified material density of 80 - 85 % TD. These nitride fuels with tailored structures will be investigated in both BOL and high burn-up irradiation experiments, accompanied with out-of-pile tests under isothermal and axial gradient conditions.

Our investigations in the last two years have shown, that it is not sufficient to specify for porous nuclear fuels only the density of the fuel pellets. The behaviour of these materials in the temperature range of their utilisation must also be well defined in order to predict their in-service properties.

Under usual sintering conditions in the temperature range of 1875 - 2000 K these materials are often still in the intermediate sintering stage with relatively high rate of densification. If the sintering process is interrupted once the specified density is obtained and the pellets thus treated are placed in a reactor, the densification process is reactivated in-pile at temperatures lower than the original sintering temperature, as has been observed in the irradiation experiments NILOC 1 and 2.

In TUAR 88 a method has been proposed by which, besides the density of the imaterial, also its behaviour at high temperatures can be quantified.

During the last month a series of fuel pellets has been prepared by variation of the consolidation procedure. The synthesised nitride reaction product, both granulate and pellets, was submitted to a thermal treatment at 1950 - 2025 K before final consolidation. Other parameters within these experiments were the pressure during pelletising and the sintering temperature.

Besides the usual characterisation by chemical and ceramographic means, the behaviour of these nitride test fuels is actually examined in the temperature range from 1875 - 2400 K both under a radial temperature gradient and under isothermal conditions.

Irradiation Experiments

Fast Reactor Experiments NIMPHE 1 and 2

The NIMPHE (TUAR 86) irradiation experiment was continued in the PHENIX reactor during the reporting period. At the end of the 5th cycle a maximum burn-up of 8 % was reached. The capsule was dismantled for intermediate examination. Nine nitride pins were discharged and are now under non-destructive examination. Depending on the results of this investigation some pins will be analysed by destructive examination in the hot cells of CEA-Cadarache and ITU-Karlsruhe.

These pins are planned to be replaced in the capsule by newly fabricated (U, Pu)N fuel pins for further irradiation together with the already irradiated fuel pins.

The NIMPHE 2 (TUAR 88) irradiation experiment, which started in October 1988 in the Phenix reactor, was continued and will reach at the end of the reporting period after 3 irradiation runs a maximum burn-up of about 4 %. Also for those fuel pins an intermediate irradiation examination is planned.

BOL-Irradiation Experiments NILOC 3 and 4

The investigation of the different fuel types at beginning of life (BOL) is continued with the irradiations NILOC 3 and 4 in the HFR, Petten.

The NILOC 3 experiment is an irradiation at standard center fuel temperatures between 1575 - 1875 K with two (U,Pu)N fuel pins and a fuel pin with an axial heterogen distribution of (U, Pu)O_2 and UN pellets.

NILOC 4 is an irradiation at high fuel centre temperatures in the range from 1925 - 2175 K. It will be designed in order to gain more information on the strong restructuring phenomenes, which have been observed in the NILOC 1 and 2 irradiations.

Tab. 1.1 shows both fuel and irradiation data for the planned experiments. The fuel and fuel pins are actually in preparation. The start for the irradiation is planned for the beginning of 1990.

Tab. 1.1 Fuel and fuel pin specification for irradiation experiment Niloc 3 and 4

Fuel Data		NILOC 3		NILOC 4
Chemical composition		(U, Pu)N	$(U,Pu)O_2$	(U, Pu)N
Pu enrichment	Pu/U + Pu		0.23	
U enrichment	$^{235}U/U$	0.83		0.93
Fuel density	% T.D.		84 ± 2 %	
C	ppm		< 1000	
O	ppm	1000<0<3000		1000<0<3000
Blanket		UN		UN
Pellet diameter	mm	5.39 - 5.51		7.10 - 7.22
Fuel stack length	mm		344	
Cladding			15/15 Ti	
Outer diameter	mm	6.55		8.50
Inner diameter	mm	5.65		7.36
Fuel to clad gap	µm		70 - 130	
Bonding			He	
Irradiation Conditions				
max. linear power	kW/m	42 - 48		71 - 87
Averaged specific power	W/g	160		155
Cladding mid-wall temp.	°C		650	
goal burn-up	a/o	1		0.5

Fire Experiments under Realistic Laboratory Conditions

Introduction

As indicated in previous reports (TUAR 87, 133 and TUAR 88, 116), a complete characterization of contaminated smoke from glove box fires requires measurement of the particle size distribution of the contaminated aerosol particles.
Such measurements were carried out in the reporting period by means of a high volume cascade impactor, in two series of standard PMMA-fires with contamination simulated (i) from powder and (ii) from solution evaporation.

The planned calibration of the high volume cascade impactor using a TSI absolute particle sizer could unfortunately not be carried out due to technical problems with the latter instrument.

Aerodynamic Size Measurements

The high volume Andersen's cascade impactor (mod. 234 SIERRA Instruments Inc.) has four impaction stages and a back-up filter (for the remaining fine particles). When operating at a nominal flow rate of 68 m^3/h, this instrument fractionates suspended particulates into five aerodynamic size fractions with calculated size cut-offs (50 % collection) of respectively 7.2 and greater, 3.0, 1.5, 0.95 and less than 0.95 µm.

The cascade impactor is directly connected to the ventilation exit channel. Care has been taken during the installation, that the connecting tube is as short as possible and that isokinetic sampling is assured by adjustment of the inlet nozzle. Whatman cellulose filters are used as collection substrate for the impaction stages and subsequently analysed (together with the back-up filter) for europium by neutron activation.

The previous observation, that the carbonaceous smoke particles are aerodynamically much smaller than the heavy metal carrying particles was dramatically confirmed during these experiments. The large excess of carbonaceous particles, which were hardly deposited on the impaction stages, tended to clog the back-up filter, so that the sampling flow rate could not be maintained during the complete course of the fire. To overcome this difficulty, the sampling is switched on exactly 5 min after the fire is started and switched off when the flow rate falls to 50 m^3/h, i.e. on an average 3 min 30 sec later. The resulting time interval corresponds to the highest rate of heavy metal spreading as shown in the time pattern of a standard fire (1), so that the amounts collected on the stages can be determined with a sufficient sensitivity. On the other hand, it is calculated that when the flow rate decreases from 68 to 50 m^3/h, the cutt-off diameters increase by about 20 %. Therefore this procedure appears to be an acceptable compromise between accuracy and sensitivity.

For maximum sensitivity, the PMMA fuel was contaminated with 150 mg of heavy metal per plate (instead of usual 75 mg), from either Eu-Ce-oxide powder or Eu-Ce-nitrate solution (see TUAR 88 p. 118). The raw results obtained from both series of experiments have to be corrected after calibration. From these raw results, presented in Tab. 1.2, the following conclusions can actually be drawn:

- For both types of contamination sources, powder or dried solution, the particles carrying away the heavy metal are independent from and substantially bigger (aerodynamically) than the carbonaceous smoke particles. This phenomenon is important for dispersion calculations involving heavy-metal contaminated smoke.

- The heavy metal carrying particles originating from PMMA contaminated with powder are significantly bigger than those from PMMA contaminated with a dried solution.

Reference

[1] K. Buijs and B.Chavane, Report EUR 11809 EN (1988)

Tab 1.2 Particle size analysis of heavy metal particles spreaded from contaminate PMMA-fires (the cut-off point values are only indicative)

Experiment Number / Cut off size D_{p50} (µm)	Cumulative mass percent of Cerium					
	Contamination from Eu-Ce-nitrate solution			Contamination from Eu-Ce-oxide powder		
	1	2	3	4	5	6
7.2	80	78	84	66	58	63
3.0	68	53	76	40	30	41
1.5	58	39	68	23	17	22
0.95	46	28	61	12	9	12

The Resuspension of Radioactive Dusts in Fires

Introduction

Experiments on the resuspension of radioactive dusts in fires were continued (TUAR 87). The dependence of the degree of resuspension on the substrate material was investigated. Previous results were obtained only for Plexiglas. The dependence of the degree of resuspension on particle size was also investigated.

Experimental

Uranium-plutonium oxide particles were obtained by abrading sintered fuel pellets in a vibrating pot aerosol generator. This oxide contained 80% U and 20 % Pu; it also contained a small amount of 241-Americium as an impurity. These particles were classified according to aerodynamic diameter in an Anderson stack cascade impactor to obtain four separate size fractions: 1.3 - 2.2 µm, 2.2 - 4.1 µm, 4.1 - 6.5 µm, 6.5 - 9.5 µm. Particles from these impactor stages were then transfered to polished steel surfaces.

The substrates chosen were those used either as constructional materials (steel, plexiglas, polycarbonate, hypalon, neoprene) or those which are commonly used inside glove boxes (PVC, polythene, cardboard). Combustible materials such as plexiglas were ignited whereas non-combustible or poorly combustible materials were exposed to flames from burning plexiglas (polycarbonate, polyethylene) or to a butane gas flame (e.g. steel). In all cases the maximum temperature of the fire was about 700 C.

Two substrates geometries were used: either disc shaped specimens 16 mm in diameter (2 cm^2 area) were cut from sheet materials (steel, PVC, plexiglas, cardboard, rubber) or samples in the form of vertical hollow cylinders 20 mm high were used (plexiglas, polyethylene, polycarbonate). The cylindrical specimens

burnt down at a constant rate like candles. Contaminant powder was applied to the upper surface of the discs of various materials or to the outer surface of the cylinders either by pressing the disc or by rolling the cylinders across the steel surfaces on which the particles from the impactor stages had been previously transfered. The amount of contaminant transferred in this way was determined by weighing to about 3 mg per sample.

A 50 cm tall combustion chamber with a 10 cm x 10 cm cross-section was installed in a glove box to enable substrates contaminated with uranium-plutonium oxide particles to be burnt or exposed to flames under controlled conditions. A constant combustion rate was achieved only in the case of hollow cylinder specimens.

The chamber was equipped with computer controlled data acquisition equipment for temperature, gas composition and specimen weight. The oxygen, carbon monoxide and carbon dioxide content of the filtered combustion gases was measured by infra-red absorption and the temperature by a vertical array of 5 thermocouples.

For aerosol sampling the chamber was equipped with vertical arrays of filter sampling ports and removable deposition surfaces. The filter samples were either taken sequentially during the fire or were left running for the whole duration of the fire. The deposition surfaces were exposed for the duration of the fire and thus provided integral values.

The fate of the contaminant in the fire was determined from the alpha activity of: a) filter samples (airborne fraction), b) sampling surfaces (wall deposition), c) a collecting surface beneath the burnt sample (particles detached but not airborne), and d) the fire residue (non-resuspended fraction). The contributions of the different nuclides to the total alpha activity was determined by alpha energy spectrometry: Pu-239 (5.15 MeV)=77 %, Am-241+Pu-238 (5.486 MeV + 5.499MeV) = 23 %. The detection limit in alpha counting, due to the background, varied from about 10^{-6} to 10^{-5} of the initial contaminant.

Results

An air flow rate of 12 l/min, corresponding to a flow velocity of 20 mm/s was used in all experiments. The fire lasted about 6 mins and reached a temperature of 600 - 700C. These data were reproducible to within 10 %. The carbon dioxide content of the combustion gases rose to about 5 % and the oxygen content fell by a corresponding amount (see Fig. 1.1). The CO content of the gas did not exceed the detection threshold of 0.01 %. The rate of combustion was essentially constant for cylindrical specimens e.g. about 0.01 g/s for plexiglas.

Both in the case of the separate size fractions, and also in the case of a log-normally distributed uranium-plutonium oxide dust with a mass median aerodynamic diameter of about 5 microns and a standard deviation of about 2, the distribution of radioactive material after a fire was typically: 75 % in the fire residue, 5 % on the floor immediately beneath and around the fire, 18.5 % on the walls and 1.5 - 2 % collected as aerosol in the exit duct. It thus appears that about 80 % of the contaminant remained in the immediate vicinity of the fire and that 20% can be transported some distance in aerosol form.

Experiments made with size fractions of the polydisperse dust taken with a cascade impactor showed little dependence of the degree of resuspension on particle size (TUAR 88, p.116).

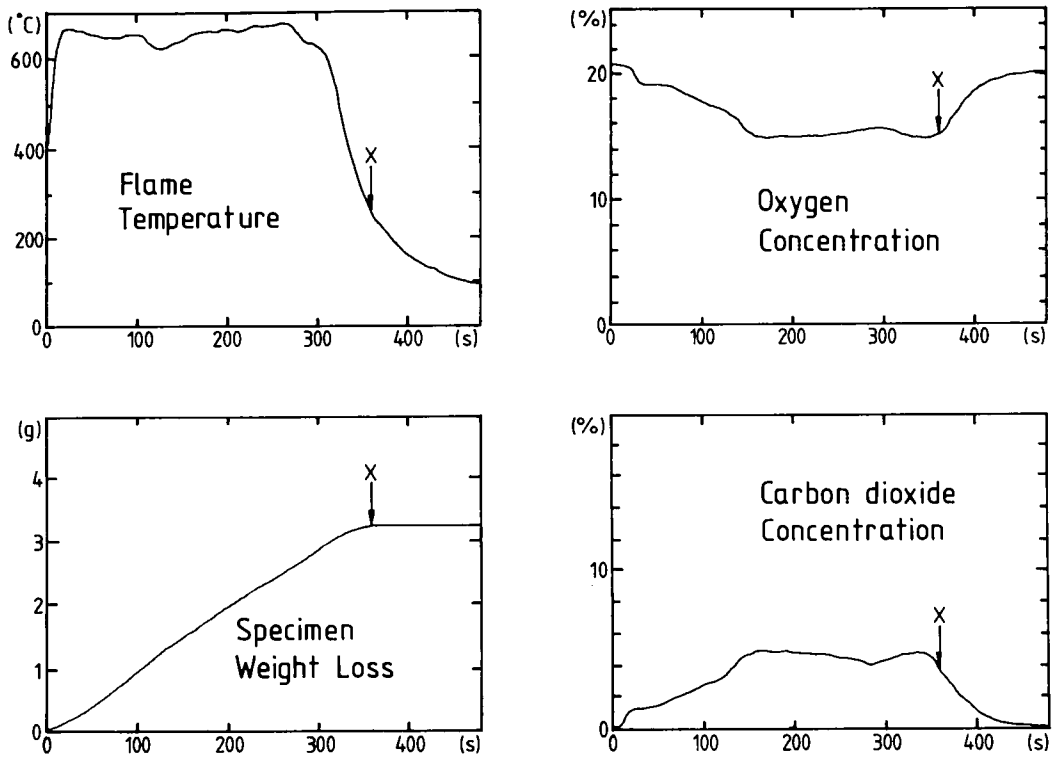

Fig. 1.1 Evolution of typical small-scale fire

It should be noted that the large particles obtained with the impactor are in fact agglomerates, if these agglomerates break up in the fire, they may be resuspended separately. Large particles, whether agglomerates or not, may also act as agglomeration centers for soot particles thus acquiring a fluffy coating which reduces their sedimentation velocity and allowed them to be transported like small particles. The possibility that large particles of uranium-plutonium oxide particle may fragment to finer particles when exposed to the oxidizing atmosphere of the flame is discounted after electron microscopy of particles before and after exposure to a gas flame at 700 C.

The resuspension of particles did not depend to any measurable degree on specimen geometry in the case of plexiglas where both disc shaped and cylindrical specimens were used.

A single experiment with a steel substrate exposed to a gas flame showed no measurable resuspension i.e. $<10^{-5}$.

A single experiment where uranium-plutonium nitrate solution was allowed to dry on a plexiglas disc to simulate a chemical spillage gave a degree of resuspension of about 10^{-4} i.e. about two orders of magnitude less than for particulate contamination.

Discussion

The results obtained in this work are compared with earlier work in Tab. 1.3 Although in large scale fires [4] much larger amounts of contaminant particles (75%) are transported within the fire room, the most interesting feature is that in

none of the experiments did more than about 3% of the contaminant remain airborne long enough to leave the fire chamber regardless of the wide variety of fire situations studied.

Combustion of Plexiglas was seen to be accompanied by extensive bubble formation just below the burning surface [3]. The bubbles, filled with pyrolysis products, nucleate some distance below the surface and then migrate up the temperature gradient to the surface where they burst. Bubble formation is a prominent feature of combustion and is regarded as a primary mechanism for particle resuspension [5].

Tab. 1.3 Comparison of results on the amount of contaminant resuspended as aerosol with data from the literature.

AUTHORS	AEROSOL	SCALE	CONTAMINANT	SUBSTRATE
This work	< 2 %	small	U-Pu 1 - 9 µm	Various
Seehars [2]	< 0.1 %	small	Pu 1 - 5 µm	Kerosene
Halverson [1]	< 3 %	small	U 1 µm	Plexiglas
Buijs et al. [4]	< 1.5 %	large	Ce/Eu <40 µm	Various

The formation of bubbles can explain why different substrates resuspend to different degrees. Polyethylene for example melts to a liquid which burns without bubbling and polycarbonate chars to a rigid surface crust. The cardboard used in these experiments was from cylindrical waste containers bonded with a resin or glue capable of bubble formation when heated explaining a degree of resuspension similar to plexiglas.

It is interesting to note that particulate matter was resuspended more efficiently than dried solution but there is no obvious reason for this difference.

Conclusions

The main conclusion is that despite the strong dependence of the degree of resuspension on the substrate material, at most 2% of the inventory of radioactive particles can be expected to be transported into the ventilation duct of a room in which a glove box fire occurs. Larger amounts of contamination (up to 75 % depending on the scale of the fire) will be spread in the immediate vicinity of the fire.

In the case of a small scale fire the main particle resuspension mechanism is bubble bursting in the substrate and the degree of resuspension depends directly on the this parameter. In large scale fires however other experiments have shown that turbulence can act as an additional resuspension mechanism.

References

[1] M.A. Halverson, M.Y. Ballinger, Trans. ANS **46** (1984) 77
[2] H.D. Seehars, J. Aerosol Sci. **14** (1983) 446
[3] S. Pickering, J. Aerosol Sci. **18** (1987) 927
[4] K. Buijs and B. Chavane de Dalmassy, EUR Report 11089en (1988)
[5] S. Pickering, Proc. 2nd Int. Aerosol Conf., Berlin 1986, p. 1061

1.1.3 Actinide Determination and Recycling

Ammonium Ions in Solutions of Dissolved Nitrides

As explained in the previous Annual Reports (see e.g. TUAR 87, 141 and TUAR 88, 119) a relatively small amount of ammonium ions is formed at the dissolution of nitride fuels in nitric acid: about 15 % of the nitride nitrogen is converted to ammonium ions. However, it would be advantageous to remove these ions from the dissolver solution before it is further treated within the Purex process.
Various methods for the destruction of ammonium ions have been tested in the frame of the subproject REPRO, (TUAR-88, 119). The reaction invoked by boiling the dissolver solution with an excess of nitrite ions has been studied most extensively.

The reaction with sodium nitrite, added to the dissolver solution either as the solid salt or as a solution, is fast and violent; gaseous NO_2 is being evolved. A good part of the reagent reacts with the strong nitric acid (6-8 M) prevailing in the solution, for which reason an excess of reagent is required. Up to a twenty-fold excess, relative to the ammonium ions present, was used. Concentrations up to 1.3 mmol/g UN were investigated, corresponding to a potential conversion of up to 35% of the nitride nitrogen into ammonium ions.

The addition as a concentrated nitrite solution was less effective than using solid crystals, in that the reaction ceased too early. The reaction using solid nitrite seems to be complete, or at least to reach the detection limit of the method used for determination of the ammonium ions (by Neßler's reagent). Under the conditions of measurements imposed by the nature of the solution the detection limit was in the order of 0.25 mmol NH^{4+} ions/g UN. The influence of the uranium present in the solution (high blank values) was considered in the application of the method.

It might thus be concluded that the addition of nitrite ions to the dissolver solution under boiling conditions provides a means to bring the ammonium ion concentration at least down to innocuous levels. The work reported here was completed in September 1989.

Determination of Neptunium by ICP-Mass Spectrometry

The determination of neptunium is difficult: because of the long half-life the specific activity is low making α and γ-spectrometry problematic and the lack of other stable isotopes rules out isotope dilution mass-spectrometry as a method.
ICP-MS relies on the total breakdown of chemical species to atoms by a plasma. The solutions of the elements of interest are nebulized and fed directly to the plasma. The atoms are ionised and analysed in a quadrupole mass-spectrometer. The discrimination of the mass-spectrometer is sufficient to allow isotopes of different masses to be measured and the total efficiency is high which ensures a sensitivity which is relatively constant between similar elements.

Two methods have been successfully employed for the determination of ^{237}Np: the first using external standards and the second using an isotope of uranium or plutonium as internal standard (normally ^{235}U or ^{239}Pu).

Np concentrations between 1 ppb and 1 ppm were employed for the external standard. The solutions containing Np and U or Pu for the internal standard method were diluted to give Np concentrations of approximately 100 to 300 ppb.

A small number of samples from the KNK IIb irradiation have been analysed by both methods. A practical limit to the ratio of ^{238}U: ^{237}Np was found of 10^5: when the ratios were higher than this interferences from the tailing of the mass 238 peak were found. Acceptable agreement was found between the two methods. It is planned to extend the tests to include a larger number of real samples.

Status of Irradiation Experiments in KNK II and the SUPERFACT Experiment

The final analysis of the mixed fuel samples from KNK IIb are continuing with special emphasis being given to the repetitions of uranium and plutonium and to measuring Np by ICP-MS. The irradiated samples for the KNK IIa experiment have not yet been unloaded from the reactor.
The delivery and analysis (PIE) of the SUPERFACT fuel pins from the PHENIX reactor have had to be delayed because the hot cells in the Institute are not yet ready.

The Application of LWR - FR Symbiosis to the Transuranium Element Fuel Cycle

Introduction

The long-term hazard of α-bearing waste from the present nuclear fuel cycle can be reduced by a factor of at least 200 by the recycling of all transuranium elements [1].

Within the constraints of existing LWR and FR technology a transuranium fuel cycle is described here, which takes into account the situation within the European Community in the year 2000. From the discharged 35000 t of spent LWR fuel accumulated up to then (Tab. 1.4) the Pu is recovered and recycled in the so-called self-generated mode in LWR's of a total capacity of 130 GWe. If Np, Am and Cm were partitioned from the highly active waste (HAW), they could be transmuted in fast reactors of a capacity of 4 GWe into fission products and Pu, which is recycled back to LWR's.

The implications of this scheme for the present fuel cycle is discussed from the point of view of:
- the make-up of Np-, Am- and Cm-bearing fuels and their irradiation behaviour
- the possible partitioning of the transuranium elements from HAW.

Arisings of Transuranium Elements in the Present Fuel Cycle

Nuclear energy generation is primarily based on uranium fuels where ^{235}U as well as ^{239}Pu and ^{241}Pu built up during irradiation in the reactor are the main energy-producing fission sources. Due to neutron capture other transuranium elements are formed, too.
For power stations operating with low enriched or natural uranium the rate of formation of ^{237}Np is less than in plants using higher enriched uranium whereas

the formation of the transplutonium elements primarily depends on the fuel exposure i.e. achieved burn-up. In some countries Pu is separated from the spent fuel and recycled in light water reactors. As indicated in Tab. 1.4 the formation of the higher transuranium nuclides will be more pronounced in this case because multiple neutron capture reactions start from heavier nuclides e.g. ^{242}Pu. The amount of ^{243}Am produced builds up to a value up to 20 times more than for the case without recycling and the amount of ^{244}Cm even further.

Tab.1.4 Accumulated U-elements in the year 2000 in the European Community assuming accumulative discharge of 35000 t spent fuel [2]

Generating capacity (GWe)	Mass of TU-element (t)			
	Np	Pu	Am	Cm
130	17	300	15	0.8

After discharge of spent fuel from a nuclear power station the transuranium element inventary will change due to decay. Over periods of a few years this mainly influences the formation of ^{241}Am from ^{241}Pu decay and the decay of the shorter lived nuclides of curium.

Transmutation of Transuranium Elements

In the following discussion the transmutation of actinides will be considered to take place in existing nuclear power stations. The half-life of a transmuted minor actinide differs considerably from the half-life of the natural decay. The transmutation half-life is determined by the neutron flux and the effective neutron cross-section and leads to transmutation into fission products or another actinide. For the existing fast reactor power station of the 300 MWe class (PHENIX, PFR, SNR-300) as well as for the larger 1000 MWe (SUPERPHENIX, EFR) the transmutation into other actinides dominates transmutation by fission. Nevertheless the overall transmutation half-life is about 3 years.
The actinides formed are mainly plutonium nuclides which can be recycled together with the Pu produced in the UO_2 matrix of the fuel thus further denaturating the LWR Pu. If a more efficient transmutation into fission products is required then a harder neutron flux is needed such as found in fast reactors with metal, carbide or nitride fuels. Remaining within the possibility of the already developed nuclear technology however, i.e. PWR with Pu recycling and FBR with MOX fuel, the following options for minor actinide recycling exist:

- recycling in PWR together with Pu
- recycling in LMFBR together with Pu
- recycling in LMFBR without Pu (which is recycled in LWR).

The minor actinides have a potential fuel value only in reactors with a fast neutron spectrum and have a reactivity at the start of the irradiation considerably lower than that of Pu . The recycling of ^{237}Np and ^{241}Am in LWR's seems feasible, since their composite half-lives (the transmutation into fission products and other actinides plus natural decay) are short. However, the transformation rate into fission products in a fast neutron spectrum of present

LMFBR design is higher and could be considerably increased if fuels other than oxides were used. More important in the case of ^{241}Am is the fact that the ^{242m}Am generated by neutron capture of ^{241}Am has an extremely high fission cross-section (in the order of 10^6b) in thermal fluxes which leads to strong neutron resonance shielding of the fuel and consequently to a pronounced anisotropic burn-up. Neutron capture reactions on the heavier minor actinides also would lead to the build-up of considerable amounts of ^{252}Cf in thermal reactors which would make the subsequent fuel handling more difficult.

If the present economic advantage of Pu recycling in LWR's is taken into account, the optimal strategy for the transmutation of transuranium elements would therefore be to recycle Pu in LWR's and to transmute Np, Am and Cm in LMFBR's.

Partitioning of Transuranium Elements

The recovery of Pu by the PUREX process does not foresee the separation of the other transuranium elements. Nevertheless several processes have been developed and tested which are capable of isolating Np and transplutonium elements, the latter, however together with some lanthanides.

In the United States, the application's of bifunctional carbamoyl methyl phosphonate have received much attention. Research efforts have concentrated recently on the development of the TRUEX process [3-5].

Intensive investigations of bi- and poly-dentate organo phosphorus and organo phosphorus-nitrogen extractants have been carried out in the Soviet Union[6-10].

In Europe, laboratory studies and hot experiments have been carried out on the HDEHP (diethyl hexyl phosphoric acid) and TBP (tributyl phosphate) extraction processes as well as the OXAL process [11-13].

A new dialkyl phosphoric acid, diisodecyl phosphoric acid DIDPA, which can extract trivalent actinides at pH~0.5 was suggested by Japanese scientists instead of HDEHP which extracts trivalent actinides only at pH 1 [14, 15]. Experiments on active solutions have proven its feasibility.

A mixed alkyl phosphine oxide was found to be a good extractant for trivalent actinides [16-18]. It extracts trivalent actinides efficiently from 0.05 - 1.5 M HNO_3.

The separation of Am/Cm from the lanthanides is a difficult task. In most systems the separation factors between trivalent Am/Cm and lanthanides are as low as those between individual lanthanides. Common systems for separating lanthanides, such as multistage solvent extraction with total reflux, or elution chromatography on cation exchangers are not favoured because of the severe radiation damage to solvent or ion-exchanger. A process employing HDEHP extraction with diethylene-triamine-pentaacetic acid stripping - the TALSPEAK process - appears still to be the only technical feasible process.

Cost/Benefit of Transuranium Element Fuel Cycle LWR - FR Symbiosis

The cost of separating and transmuting the minor actinides (MA) in fast reactors has been estimated at 2 to 4% of the electricity generating cost of a FR [19, 20] (which at present is considerably higher than that of a LWR). The additionally generated energy from MA transmutation would be 4% [1], which would compensate for the cost in a FR economy. Moreover the presence of MA in a FR fuel would extend the reactivity of fuels with a corresponding extension of the fuel cycle.

A 200 fold reduction of the α-radiotoxicity of the nuclear waste is achievable with present technology. Improvements are still possible as outlined in the proposals for the Omega project by the Japanese Government.

References

[1] L. Koch, "Minor Actinide Transmutation - A Waste Management Option", J. of the Less-Common Met. **122** (1986) 371-382
[2] "Summary of Nuclear Power and Fuel Cycle Data in OECD Member Countries", Nuclear Energy Agency (1986)
[3] G.F. Vandegrift, R.A. Leonard, M.J. Steindler, E.P. Horwitz, L.J. Basile, H. Diamond, D.G. Kalina, L. Kaplan, ANL-84-45 (1984)
[4] E.P. Horwitz, D.G. Kalina, H. Diamond, L. Kaplan, G.F. Vandegrift, R.A. Leonard, M.J. Steindler, W.W. Schulz, Actinide/Lanthanide Separations", Ed: G.R. Choppin, J.D. Navratil and W.W. Schulz, World Scientific Publication, Singapore, (1985) 43
[5] E.P. Horwitz, D.G. Kalina, H. Diamond, G. Vandegrift, W.W. Schulz, Solvent Extr. Ion Exch. **3** (1985) 75
[6] B.F. Myasoedov, Solvent Extr. Ion Exch. **4** (1986) 61
[7] M.K. Chmutova, N.E. Kochetkova, B.F. Myasoedov, J. Inorg. Nucl. Chem. **42** (1980) 897
[8] B.F. Myasoedov, Solv. Extr. Ion Exch. 1, (1983) 689
[9] A.M. Rozen, Z.I. Nikolotova, N.A. Kartashera, Radiokhimiya **28** (1986) 40
[10] A.M Rozen, Proc. Inter. Solv. Extr. Conf. '88 (1988) 133
[11] F. Mannone, H. Dworschak (eds.), Chemical Separation of Actinides from High Activity Liquid Wastes, Final Report, JRC Ispra, S.A./1.07.03.84.02 (1984)
[12] J.O. Liljenzin, G. Persson, I. Svantesson, S. Wingefors, Radiochimica Acta **35** (1984) 155
[13] G. Persson, S. Wingefors, J.O. Liljenzin, I. Svantesson, Radiochimica Acta **35** (1984) 163
[14] M. Kubota, H. Nakamura, S. Tachimori, T. Abe, H. Amano, IAEA-SM-246/24 (1981)
[15] M. Kubota, I. Yamaguchi, K. Okada, Y. Morita, K. Nakano, H. Nakamura, Mat. Res. Soc. Symposium Proc. **26** (1984) 551
[16] Zhu Yongjun, Jiao Rongzhou, Wang Shouzhong, Fan Shiguo, Liu Bingren, Zeng Hualing, Zhou Shunli, Chen Shuming, Proc. Inter. Solv. Extr. Conf '83 (1983) 9
[17] Jiao Rongzhou et al., Chinese J. Nucl. Radiochem. 1 (1985) 65
[18] Zheng Hualing et al., Chinese J. Nucl. Sci. Eng. **5** (1985) 147
[19] J.O. Blomeke, A.G. Croff, B.C. Finney and D.W. Tedder, EUR 6929 (1980)
[20] E. Schmitt, E. Zamorani, W. Hage and S. Guardini, S.A., JRC Ispra S.A./1.05.03.83.13 (1984)

1.1.4 Characterisation of Waste Forms and High Burn-Up Fuel

The studies on radioactive wastes carried out at the Institute for Transuranium Elements are centered on the characterisation of the waste forms (mainly unprocessed spent fuels and vitrified high level wastes), with respect to properties relevant to their behaviour under conditions of long term storage.

Properties to be investigated include radioactive nuclide inventory, thermal conductivity, thermal and mechanical stability, redistribution of actinides and fission products within the waste materials, radiation damage, resistance to corrosive agents and investigation of the leaching behaviour with various leachant compositions.

While during the present exercise the installation for use at the hot cell level of various equipments for physical measurement and chemical analysis was continued, specific results were obtained as summarized below.

Spent Fuel Characterisation and Related Studies

Leaching, Hydration, and Surface Analysis of Unirradiated UO_2

To provide basic data necessary for any model of leaching of spent fuel, the leaching of unirradiated UO_2 and of UO_2 with an impurity composition simulating a given burn-up are useful. Such experiments have already been performed on UO_2 using water and salt brine (Q-brine) in the temperature range of 20 to 200 °C for time periods of up to 3 months. To determine extent, depth and kinetics of surface layers formed on UO_2, sensitive nuclear methods had to be developed and used . Rutherford backscattering and the channeling technique were used to measure thickness and U-content of surface layers, and elastic recoil detection analysis (ERDA), was employed to determine possible hydrogen uptake.

The results show that leaching of UO_2 in water for the above conditions leads to the formation of a U_3O_7 layer with a maximum thickness of a fraction of a µm. This layer contains no measurable hydrogen and its growth is not diffusion-controlled, but rather control by a reaction on the interface UO_2/U_3O_7 is indicated. Further oxidation is influenced by redeposition of uranium from the solution. At 200 °C, thick layers of hydrated UO_3 are formed. Their water content is smaller than that of the thermodynamically expected composition of schoepite ($\sim UO_3 \cdot 3H_2O$). The non-destructive analysis of hydrogen depth profiles by ERDA was, for the first time, shown to be a suitable means to study hydration of UO_2.

Initial results in Q-brine indicate formation of surface layers containing salt components. First results in water with the pH-value as parameter indicate an interesting influence of pH.

Similar measurement on UO_2 fuel with simulated burn-up have also been undertaken and the first results are just becoming available. Future experiments will have the aim to provide detailed information on these two parameters.

Characterization of UO_2 and MOX Spent Fuels

Preliminary leaching tests on used UO_2 and MOX fuel pieces as waste forms have been conducted since March 1989 by means of Soxhlet extractors for durations of 7, 30 and 100 days, according to the MCC-5S test procedure using doubly distilled water as leachant. Ultimately, these leaching experiments will be carried out in autoclaves in which whole segments of fuel rod with deliberate defects, pieces of cladding material, and fuel pellets will be exposed to doubly distilled water (and also brine and groundwater).
This study will be focussed on fuels relevant to the European technology, i.e., UO_2 irradiated at high burn-up and MOX fuels of thermal reactors.

The objectives of the present study are:

- to evaluate the release of radionuclides including U, Pu and TPu elements from fuel and cladding into doubly distilled water under dynamic conditions. In the former case the release will be studied as a function of the fuel location (e.g. outer rim and central part of the pellet).

- to characterize before and after leaching the surface microstructure of the fuel (and radial cracks) as a function of their location.

- to compare these microstructures with that of the fuel matrix

- to determine how the corrosion proceeds.

Given here are the results obtained from the 30 day leaching tests. The burn-up reached was 31.5 and 38.8 GWd/T_U for the UO_2 and MOX specimens, respectively.

5 specimens have been simultaneously leached in Soxhlet extractors of the type described in TUAR 88, p. 176.

The two UO_2 and two MOX specimens have been selected from decladded fuel pellets. They are segments representative either of the central part or the outer part of the fuel pellet. The fifth specimen is a piece of cladding from the UO_2 fuel.

a) Fuel outer surface microstructure

1) Before leaching

In comparison with the UO_2 matrix microstructure the surface of the outer rim and radial cracks of the as irradiated fuel pellet showed some of the structural features found in the matrix but also specific ones that are described hereafter:

At the outer rim surface the microstructure differs from that of the matrix by the absence of interaction between UO_2 and Cs, a more dense structure and the presence of crystalline deposits (UO_2) and platelet-like crystals grown on the grain surface that are suspected to be U_4O_{9-x}. [1]

At the radial crack surface the fracture mode is mainly intergranular in the colder region, but evolves to the transgranular/intergranular mode when moving to the hotter region. Crystalline deposits are visible but less frequently than in the outer rim; the U_4O_{9-x} phase was detected as well. At intermediate radial position eroded structures were observed. In the hotter part metallic fission products (Mo, Rh, Ru, Tc, Pd) and pores are precipitated either on the grain faces or within the grains.

2) After leaching

The most important change is the disappearance of the platelet-like phase (U_4O_{9-x}) and of the crystalline deposits. The microstructure yields evidence of localised corrosion pitting and supports the idea that corrosion proceeds not only at grain boundary but also at preferential sites of grain or grain fracture surface where the grain microstructure is affected by the precipitation of metallic fission products or by porosity.

b) Cladding microstructure

1) Before leaching

Besides the expected discontinuous oxidation of Zircaloy two supplementary chemical interactions were determined:

a. The crystalline UO_2 deposits on the inner side of the cladding interacted with Zr. U diffusion into Zr was observed with simultaneous formation of an oxide. Cs reacted with this oxide to form a Cs (U, Zr) O compound. The size of individual formations of this phase can exceed a few hundred microns.

b. The ZrO_2 phase sometimes contained additional elements such as impurities of the fuel (Ca, Cl, Si) or fission product (Cs) as well as U. As no evidence was found for the formation of specific compounds the expected interaction between Cs and I or Te could not be demonstrated.

2) After leaching

It appears that Cs, Si, Cl and Ca are released from the phases described above.

Reference

[1] B.E. Schaner, J. Nucl. Mat. 2 (1960) 110-120

Non-Destructive Assay of Spent Nuclear Fuel

The purpose of the assay is to verify a declaration of the fissile/minor actinide content in spent fuel and to determine its burn-up and cooling time. The following ND techniques have been surveyed in the literature: passive (gamma-ray spectroscopy of fission products, neutron counting both gross and by coincidence), and active (prompt neutron counting by coincidence, delayed gross neutron counting, prompt and delayed gammas). The implementation of these techniques in a hot-cell is being investigated. Since interpretation of the measured signatures is more effectively achieved through isotopic correlations techniques, the depletion code KORIGEN is being used to simulate correlations between the signatures to be measured and the parameters of the fuel to be determined. Useful correlations have been established relating ratios of fission products activities and/or neutron signals with fissile material and minor actinide content, long-lived fission products (^{129}I, ^{99}Tc), burn-up and cooling time.

Characterisation of Vitrified High Level Wastes and Related Studies

Conclusion of the Studies on Alpha Radiation Damage using ^{244}Cm Doped Glasses

The three HLW glasses (French SON 68.18.17 L1C2A2Z1, American MCC 76-68 and German GP 98/12) doped with 0.5 and 1.5 wt.% ^{244}Cm to accelerate realistically damage formation have reached saturation damage. Final measurements of volume changes, crack behaviour and fracture toughness as well as leach rates were made.

The volume changes were very small ($\leq$ 0.6 %). Both negative (shrinkage) and positive changes (swelling) were observed. No obvious relation with glass type or damage rate could be seen. The leach rates did not increase with increased damage level, in contrast to glasses damaged with external particle beams. There was rather a tendency towards a small decrease in leach rates. The fracture toughness increased significantly in damaged glasses, a positive phenomenon for technical application of the glasses.

The parallel work on damage formation by controlled ion implantation was extended to damage production at different elevated temperatures up to 450° C. Damage with external charged particles increases the leach rate of the glasses and causes changes in the Na distribution by biased radiation-enhanced diffusion in the electric field set-up by the ion beam. The results show a previously unknown difference in damage recovery: the chemical changes produced by radiation persist to much higher temperatures (~450°C) than the changes in fracture toughness. These are due to damage induced stresses and are largely absent for damage production at T $\geq$ 250° C.

Characterisation of Highly Active Waste Glasses

The present report concludes the characterisation, initiated in 1987, of highly active waste glasses of the ESTER experiment (collaboration with ENEA COMBSVITE and JRC-ISPRA). We report here the electron microprobe analysis of the gel layers after leaching. A short discussion of the various experimental results and the conclusions drawn are also presented. A continuation of this task is foreseen in connection with the availability of fully active waste glasses from the PETRA installation at JRC-Ispra.
Information concerning the microstructural analysis (before and after leaching), leaching tests, leachates analysis and quantitative metallography can be found in TUAR-87, pp. 210-213 and TUAR-88, pp. 173-178.

Sectioned glass specimens were impregnated in epoxy resin, for analysis with the electron microprobe to obtain information on the composition of the altered layer after the corrosion tests. The experimental results showed that the matrices had mainly the same composition as before corrosion, with the gel-layers having very low concentration in the glass constituents, particularly Si, and a strong depletion in Mo and Cs. On the other hand, the gel-layers appeared enriched in transition metals and rare earths. Some elements (e.g., Ce, Gd, Zr, Nd, Ti, Cr) were present mainly in the inclusions which remained trapped in the altered layer, as confirmed by X-ray mapping of the corresponding areas. In Fig. 1.2 the microprobe line scans for different elements in the glass matrix as well as in the gel layer of crucible 4 are presented.

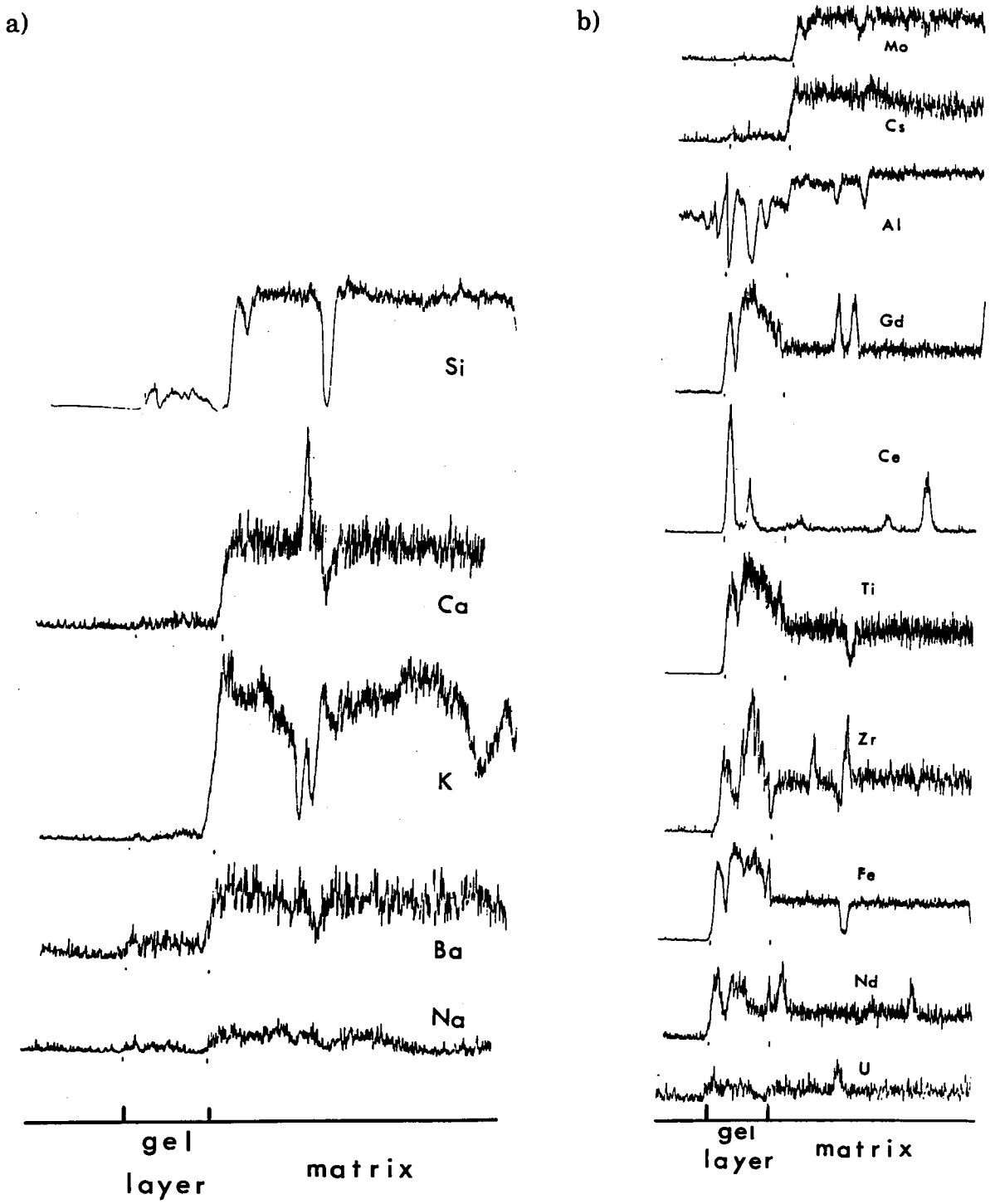

Fig. 1.2 Microprobe line scans across the surface layer formed during corrosion in crucible 4. a) glass matrix elements, b) waste elements

Discussion

1. During leaching the pH-value of the solutions showed an increase of about 1 unit for all the samples (from 6.5 to about 7.5), indicating a preferential dissolution of the alkali metal elements. This was confirmed by the chemical analysis of the leachates, where the glass constituents (in particular Si, as revealed by ICP-OES analysis) were found. On the other hand, actinides (U) and rare earths, if present, were below the detection limits. The presence of Mo and Cs in the leachates also confirmed the depletion of these elements in the gel-layers established by EDAX and electron microprobe analysis. Moreover, the increase in the solution pH indicates also that radiolysis was not significant for the total mass

losses observed, since radiolysis reduces the solution pH, as already demonstrated in previous studies.

2. Differences associated with the sample location were apparent. The elemental concentrations of the leachates from the different sections were dissimilar: some elements (e.g., B, Cs, Li and Mo) showed a higher leaching rate from the samples located at the bottom of the glass crucibles, while others (e.g., Al and Sr) were more uniformly removed from the different positions. The variations in leach rate may perhaps be due to inhomogeneities in the sample due to production procedure. This effect was more pronounced in crucible 6. No differences were found between samples taken from the center and edge of the slices, except for B and Li in crucible 4.

The chemical analysis of the leachates showed also that the leaching, depending on the element considered, seems to occur in at least two different ways: (a) the major glass constituents are leached from the surface congruently, leaving a gel network; and, (b) some metals (e.g., Ti,Zr,Fe and partially Al), rare earths and actinides, present at the beginning, - partially as inclusions -, are removed from the bulk at a slower rate and remain trapped in the gel-layer. There was some evidence that other elements (e.g., Cs and Mo) are also leached from beneath the gel/matrix boundary. Although these indications are not fully conclusive, they suggest a diffusion mechanism for leaching.

3. Corrosion tests were conducted in the past by ENEA with simulated glass products having the same matrix chemical composition and waste loading. The comparison revealed a similar dissolution behaviour for crucible 4, but in the case of crucible 6 the simulated samples showed mass losses much higher than the real glasses, indicating a beneficial effect of active waste but no explanation could be found for this effect.

4. Influence of the composition, waste loading and devitrification: since parameters such as chemical composition of the glass matrix and waste loading have not been investigated systematically in the framework of the present study, no conclusions can be drawn about the influence of the amount and type of waste oxides or glass constituents. Nevertheless, it is believed that the greater loading of crucible 4 and the relatively low Si content, are responsible for the devitrification process observed and the enhanced leach rate. Moreover, the presence of devitrified zones (inclusions) seems to be responsible for the observed root-like microcracks formation, with the inclusions forming sites for preferential attack.

Conclusions

From the various results it can be concluded that:

- the extent of the leaching depends on the element considered and occurs in different ways:

(1) the major glass network elements are leached from the surface in a congruent manner.

(2) other elements are leached from beneath the gel/matrix interface (e.g., Cs), suggesting that a diffusion mechanism is operative.

(3) some metals, rare earths and actinides, are removed from the bulk at a slower rate and remain trapped, - partially as inclusions -, in the altered layer formed during the dissolution process.

- considering the small masses leached, radiolysis effects seem to be negligible in short term testing. Further work is in progress to analyse its influence during prolonged leaching tests.

Characterisation of Cement Products Resulting from the OXAL-ILLW Exercice

As explained in the previous annual report (TUAR-88, pp.151-154) the mother liquor from oxalate precipitation of the actinide/lanthanide elements in intermediate level liquid waste solutions (ILLW), has been solidified in cement to provide specimens for characterisation of the final product. A special aim was to evaluate the influence of the excess oxalic acid on the quality of the product. Non-active as well as active samples have been considered. The work has been completed and the final report is under preparation.

Consistently, it was found that the influence of oxalic acid in the concentration range studied, up to 0.3 M, was negligible, Fig. 1.3 shows as an example the compressive strength of a series of specimens as a function of time.

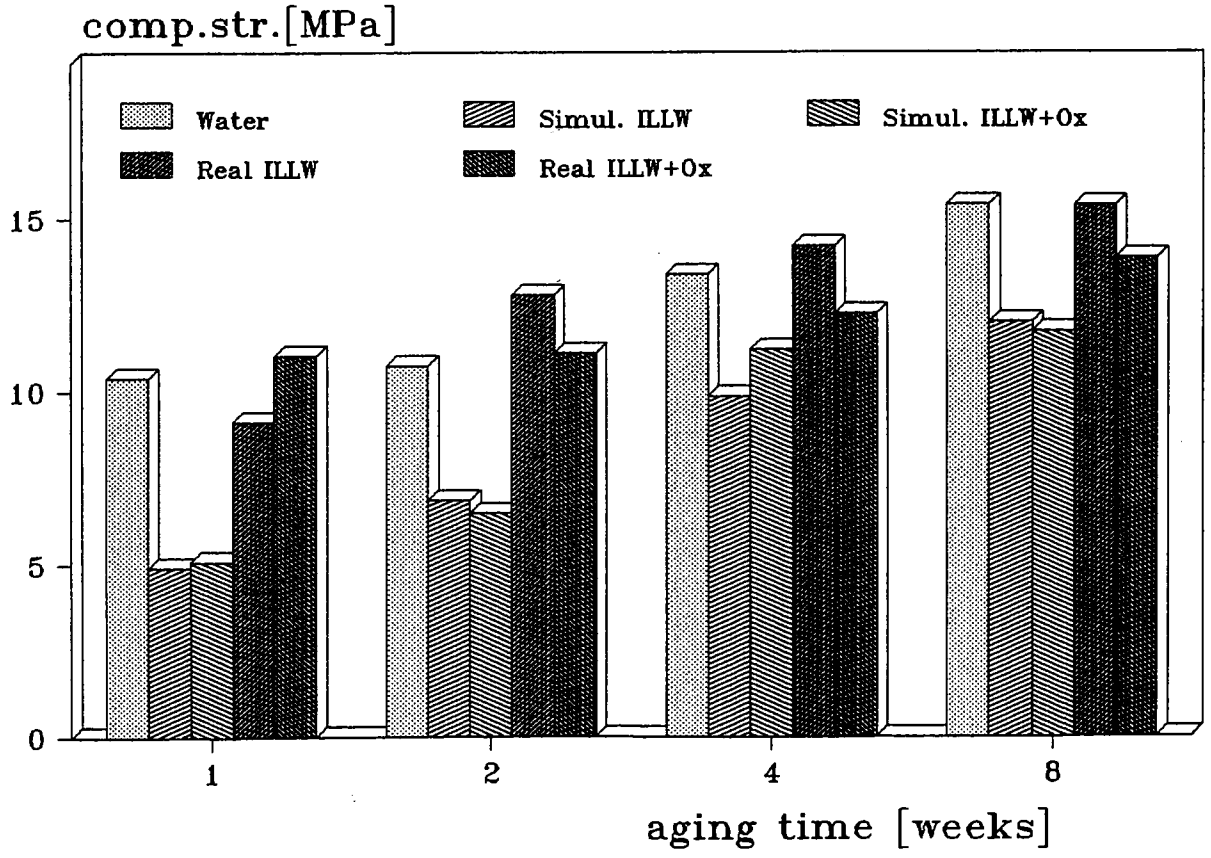

Fig. 1.3 The compressive strength of cemented specimens as a function of aging time under five different conditions

No significant difference could be found between the real active samples and the inactive simulated samples after 8 weeks of aging; if anything, the active specimens, from the particular batch of ILLW considered, were stronger than those

made from the simulated solutions. The standard deviation of these measurements, done in triplicate, was about 10 %.

A further important result was the rather high leach rate found for nitrate ions: about 30 % was lost to the leachant after 32 weeks of leaching in water at ambient temperature. The other constituents showed much higher resistance against leaching: about 1% of the initial content of calcium was dissolved under the above conditions; the corresponding values for Al and Si being 1.9 % and 0.1%, respectively.

With oxalate present in the cement the oxalate concentration in the leachant was close to the detection limit of ion chromatography (1 ppm) after 16 weeks of leaching.

These analytical determinations were carried out by ICP-OES and ion chromatography (anions). The fission products leached (mainly Cs and Eu) were determined by gamma spectroscopy.

It was found in many cases, that the presence of oxalate in the cement actually reduced the release of ions to the leachant; this behaviour was typical for calcium.

In addition, it was invariably found that the addition of 5% microsilica to the cement improved the mechanical as well as the chemical stability of the cement preparation.

It might thus be generally concluded that the possible adverse effects of the oxalate ions on the cement matrix is not significant in the range of interest for the oxalic acid precipitation, as discussed here.

1.1.5 Actinide Research

Summary and Objectives

Summary

As in previous years, the preparation of chemically pure, single phase, and well characterised compounds of actinides of high specific activity was a basis not only for solid state physics work in ITU, but also in a wide variety of collaborations with external laboratories. Single crystals were grown from part of these compounds. The accent this year was on ternary compounds of neptunium or plutonium with silicon or germanium, and a transition metal as the third component. 28 of these compounds were prepared and crystallographically characterised for the first time.

The study of the catalytic activity of nickel-actinide compounds was extended to the compounds UNi_5 and $ThNi_5$, whose apparent activation energies were determined.

The magnetic form factor of Np in $NpCo_2$ was theoretically and experimentally determined. It shows a large orbital contribution to the magnetic moment. The relative sizes of spin and orbital contributions can be explained by 5f hybridization.

Calculation of the cohesive properties from first principles indicates that lawrencium is not a simple sp metal, but the first member of a 6d transition series.

Study of the electronic levels of PuSe by photoelectron spectroscopy indicates that this compound is a high-temperature Kondo system. No experimental evidence was found for PuSe being a relativistic semiconductor.

The same compound was found to transform to a rhombohedral phase around 20 GPa and to the B2 type structure around 35 GPa. New high-pressure structures were also determined for U(P,S) and for the dioxides ThO_2 and PuO_2. The δ phase in the U-Np system showed extraordinary stability to pressure up to 62 GPa; this result is an important contribution to the refinement of the previously established diagram of the phase relations of the actinide metals. The reference diagram for the 4f elements was completed by a high-pressure study of promethium, the only lanthanide that had not yet been investigated under pressure.

Objectives

The central objective of actinide research in ITU as well as in its numerous collaborations is elucidation of the electronic structure of actinide metals and actinide compounds, in particular of the behaviour of the 5f electrons. The dualism between localized and itinerant characteristics as it is particularly clearly demonstrated in the actinide series, is a key problem in these studies.

These goals are approached by experiment and theory. Experimental study is either selective investigation on the basis of theoretical or other experimental information that indicates the particular material and method are promising, or can also be systematic study of a whole class of compounds. Theoretical calculations can indicate to the experimentalist where he can expect to find important results,

and on the other hand try to combine experimental evidence from different sources into a general picture. An important basis for the experimental study is the preparation of polycrystalline and single crystal samples of actinides of high specific activity, and their careful characterisation by x-ray diffraction, electron microscopy, and electron microprobe analysis.

Preparation and Characterisation of Actinide Metals and Compounds

Introduction

Materials preparation includes the application of a number of established techniques as shown in Tab. 1.5 and the development of new techniques for preparing single crystals of intermetallic compounds. Characterisation techniques include X-ray diffraction, electron microscopy and electron microprobe analysis.

Progress in Material Synthesis and Characterisation

Material preparation includes the systematic single crystal growth of materials forming large families of cubic isostructural compounds to allow a systematic and comparative investigation of the physical properties and the preparation of new compounds with properties of interest for fundamental and applied research.

The compounds prepared and encapsulated for physical property measurements during 1989 are listed in Tab. 1.5.

Preparation of single crystals of compounds with the NaCl structure type (monopnictides and monochalcogenides) was continued. Single crystals of neptunium sulfide were prepared for the first time, completing the neptunium monochalcogenide series. The effort on the synthesis of solid solutions of neptunium compounds was continued with the preparation of single crystals of $NpAs_{1-x}Se_x$ ($x = 0.05, 0.1$).

In order to prepare single crystals of new actinide pnictides, the mineralization technique was employed to synthesize An_4X_3 or An_3X_4. During attempts to prepare U_4Sb_3, single crystals up to 10 mm^3 with hexagonal shapes were obtained (Fig. 1.4). These single crystals were identified by full structure determination as U_5Sb_4 that crystallizes in the hexagonal system, space group $P6_3/mcm$ with lattice parameters $a = 924.8(3)$ pm and $c = 622.3(3)$ pm. This phase had been described in the early investigations of the U-Sb system by Beaudry and Daane [1], but its composition was given as U_4Sb_3 by these authors.

As the ternary compounds of rare-earths and actinides are the subject of intense research in the field of magnetism, heavy fermions and superconductivity, several actinide ternary intermetallics AnM_2X_2 (An = actinide, M = transition metal, X = Si, Ge) were prepared by arc-melting stoichiometric mixtures of the constituents. Powder and single crystal X-ray diffraction analysis shows that most compounds crystallize in ternary derivatives of the $BaAl_4$ type structure of the tetragonal $ThCr_2Si_2$ or $CaBe_2Ge_2$ type. The crystallographic data of the new AnM_2X_2 intermetallic compounds are given in Tab. 1.6. The full structure determination on single crystals isolated from the cooled melt by mechanical fragmentation shows that some compounds AnM_2X_2 containing transition metals of higher periods (Mo, Tc, Ru and Re) adopt a composition different from the starting stoichiometry. The crystallographic data of the new actinide ternary intermetallics are reported in Tab. 1.7.

Tab. 1.5 Samples prepared, characterized and encapsulated in 1989 for the measurements indicated

Magnetization	ETH Zurich	$NpSb_{0.90}Te_{0.10}$	M-SC
		$NpSb_{0.85}Te_{0.15}$	M-SC
		$NpAs_{0.95}Se_{0.05}$	M-SC
Neutron Scattering	ILL Grenoble	US	M-SC
		$HoFe_2$	Cz-SC
		NpAs	M-SC
		$BaAmO_3$	Powder
	CEN Saclay	$U(C_5H_5)_3Cl$	Powder
		$U(C_5H_5)_3Br$	Powder + SCS-SC
	Riso Nat. Lab.	$NpCo_2$	Cz-GSC
	Rutherford-Appleton Laboratory	UN	Powder
Moessbauer Spectroscopy	CRN Strasbourg	$NpSb_{1-x}Te_x$ (x = 0.1, 0.15, 0.2, 0.25)	GSC-Powder
		$NpAs_{1-x}Se_x$ (x = 0.05, 0.1)	GSC-Powder
		NpS	GSC-Powder
		$NpPd_2Si_2$	AcM-Powder
		$NpIr_2Si_2$	AcM-Powder
		$NpPt_2Si_2$	AcM-Powder
		$NpAu_2Si_2$	AcM-Powder
		$NpMn_2Ge_2$	AcM-Powder
		$NpRh_2Ge_2$	AcM-Powder
		$PuIr_2Si_2$	AcM-Powder
		$Np_2Tc_3Si_4$	AcM-Powder
		$Np_2Mo_3Si_4$	AcM-Powder

M = Mineralization
Cz = Czochralski
AcM= Arc Melting

GSC = Ground Single Crystals
SC = Single Crystals
Poly= Polycrystalline Material

Tab. 1.6 Crystallographic data of new AnM_2X_2 intermetallic compounds

Compounds	Space group	Structure type	Lattice parameters (pm)		c/a	Volume (nm^3)
			a	c		
$ThTc_2Si_2$	I4/mmm	$ThCr_2Si_2$	419.02(4)	1006.8(2)	2.403	0.17677
$NpPd_2Si_2$	I4/mmm	$ThCr_2Si_2$	411.26(6)	1004.4(1)	2.442	0.16988
$NpIr_2Si_2$	P4/nmm	$CaBe_2Ge_2$	409.24(2)	983.96(9)	2.404	0.16479
$NpPt_2Si_2$	P4/nmm	$CaBe_2Ge_2$	419.49(5)	975.4(2)	2.325	0.17164
$NpAu_2Si_2$	I4/mmm	$ThCr_2Si_2$	424.22(8)	1027.5(3)	2.422	0.18491
$PuCr_2Si_2$	I4/mmm	$ThCr_2Si_2$	391.33(2)	1065.79(8)	2.724	0.16321
$PuMn_2Si_2$	I4/mmm	$ThCr_2Si_2$	393.13(4)	1044.4(2)	2.657	0.16141
$PuFe_2Si_2$	I4/mmm	$ThCr_2Si_2$	393.37(2)	988.1(2)	2.512	0.15290
$PuCo_2Si_2$	I4/mmm	$ThCr_2Si_2$	390.50(2)	981.3(1)	2.513	0.14964
$PuNi_2Si_2$	I4/mmm	$ThCr_2Si_2$	397.04(3)	964.8(2)	2.430	0.15209
$PuRu_2Si_2$	I4/mmm	$ThCr_2Si_2$	415.14(4)	966.2(1)	2.327	0.16651
$PuRh_2Si_2$	I4/mmm	$ThCr_2Si_2$	403.96(5)	1006.2(1)	2.491	0.16420
$PuPd_2Si_2$	I4/mmm	$ThCr_2Si_2$	414.77(6)	996.4(2)	2.402	0.17141
$PuOs_2Si_2$	I4/mmm	$ThCr_2Si_2$	412.45(5)	978.5(1)	2.372	0.16646
$PuIr_2Si_2$	P4/nmm	$CaBe_2Ge_2$	411.15(4)	984.9(1)	2.395	0.16649
$PuPt_2Si_2$	P4/nmm	$CaBe_2Ge_2$	420.11(2)	978.5(1)	2.329	0.17270
$PuAu_2Si_2$	I4/mmm	$ThCr_2Si_2$	424.96(9)	1021.3(4)	2.403	0.18444
$NpMn_2Ge_2$	I4/mmm	$ThCr_2Si_2$	400.94(3)	1082.3(2)	2.699	0.17398
$NpRh_2Ge_2$	I4/mmm	$ThCr_2Si_2$	412.65(8)	1010.2(4)	2.448	0.17202

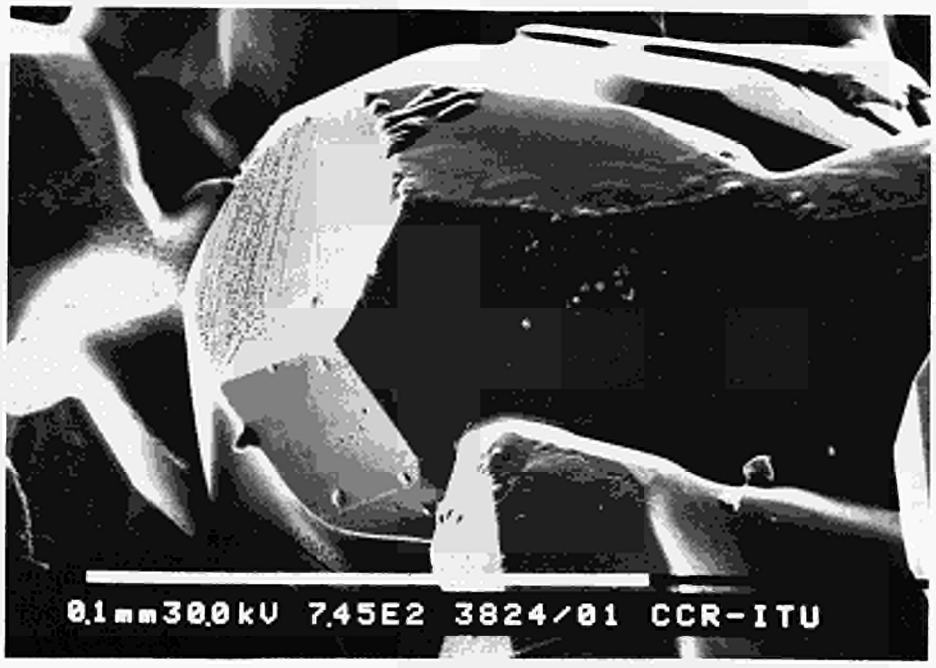

Fig. 1.4 Scanning electro micrograph of single crystals of U_5Sb_4

Tab. 1.7 Crystallographic data of new actinide-based ternary compounds

compounds	Space group	Structure type	Lattice parameters (pm)	Z	Volume (nm^3)
$U_2Mo_3Si_4$	$P2_1/c$	$Ln_2Mo_3Si_4$	a = 687.6(1) b = 688.3(1) c = 676.0(1) β = 109.79(1)°	2	0.30106
$U_2Mo_3Ge_4$	$P2_1/c$	$Ln_2Mo_3Si_4$	a = 670.0(1) b = 699.6(1) c = 694.8(1) β = 110.09(2)°	2	0.30580
$Np_2Mo_3Si_4$	$P2_1/c$	$Ln_2Mo_3Si_4$	a = 686.8(3) b = 687.7(3) c = 675.4(2) β = 109.68(3)°	2	0.30036
$Np_2Tc_3Si_4$	$P2_1/c$	$Np_2Tc_3Si_4$	a = 680.8(1) b = 808.1(1) c = 556.7(2) β = 103.61(2)°	2	0.29770
$Pu_2Tc_3Si_4$	$P2_1/c$	$Np_2Tc_3Si_4$	a = 684.3(1) b = 807.2(1) c = 558.1(1) β = 103.47(1)°	2	0.29981
$U_2Tc_3Si_5$	P4/mnc	$U_2Mn_3Si_5$	a = 1085.6(1) c = 553.1(1)	4	0.65184
$Pu_2Re_3Si_5$	P4/mnc	$U_2Mn_3Si_5$	a = 1092.9(7) c = 553.5(3)	4	0.66112
$U_4Tc_7Ge_6$	Im3m	$U_4Re_7Si_6$	a = 820.57(3)	2	0.57610
$Np_4Ru_7Ge_6$	Im3m	$U_4Re_7Si_6$	a = 831.51(3)	2	0.57492

Reference

[1] B.J. Beaudry and A.H. Daane, Trans. Met. Soc. AIME 215 (1959) 199

Catalytic Activity of Actinide - Nickel Compounds in the Hydrogenolysis of Ethane

The studies on Ni, UNi_2 and UO_2 -supported Ni, described in the previous report (TUAR 1988) were continued and extended to UNi_5 and $ThNi_5$.

The higher catalytic activity of UNi_2 with respect to that of Ni could be attributed mainly to the larger specific surface of UNi_2, as proven by BET surface area measurements.

From the partial reaction orders of ethane and hydrogen the composition of the surface intermediate in the rate determining step of the hydrogenolysis reaction was calculated to be C_2H_4 on Ni and C_2H_2 on UNi_2 and UO_2/Ni. This indicates an increase in the chemisorption bond strength between carbon and the catalyst from nickel to the uranium containing catalysts.

For UNi_5 and $ThNi_5$, the apparent activation energies were determined as 185.0 and 185.8 kJ/mol, respectively, that is about the same value as found for UNi_2 (183.3 kJ/mol). The surface intermediates for both catalysts were found to be C_2H_4, which indicates a shift of the chemisorption bond strength towards that of pure nickel due to the higher nickel content.

Solid State Physics Studies on Actinide Systems

Neutron and X-ray Synchrotron Scattering

The newest, and both fundamentally and practically important, aspect of actinide research is the realisation [1] and subsequent experimental verification of the existence of very large orbital contributions to the magnetic moments [2] in compounds where the 5f electrons are itinerant. Following the neutron diffraction studies on UFe_2, reported last year, we have made similar - both experimental and theoretical - studies of $NpCo_2$. The magnetic form factor of Np was both calculated and measured and the results found to be in excellent agreement. The measured form factor is shown in Fig.1.5 and is unambiguously due to the existence of a large orbital moment which is larger than the spin moment. We emphasise that a form factor of the shape shown could not be obtained from the type of magnetism normally found in either rare earths or transition metals. The shape is due to the relative sizes of spin and orbital contributions to the moment at the Np site, which are in turn due to the hybridizing 5f electrons.

Structural studies have concentrated upon firstly organometallic compounds with the observation of structural transitions in $U(C_5H_5)_3Cl$ and its bromide analogue and secondly upon the positions of the oxygen atoms in CmO_2.

Neutron inelastic studies of single crystals of UTe have given detailed information about the extent of hybridization between the 5f and conduction electrons. Reasonable agreement has been obtained between experiment and theory with respect to the dispersion anisotropy, and damping of the magnetic excitations.

High-energy inelastic neutron studies have been performed on a polycrystalline sample of PuO_2 and the first excited crystal-field state (at 120 meV) has been identified. Whereas its position in energy is consistent with the systematics established for UO_2 and NpO_2, this is inconsistent with the value derived from magne-

tic susceptibility measurements. Theoretical efforts to reconcile this contradiction are in progress.

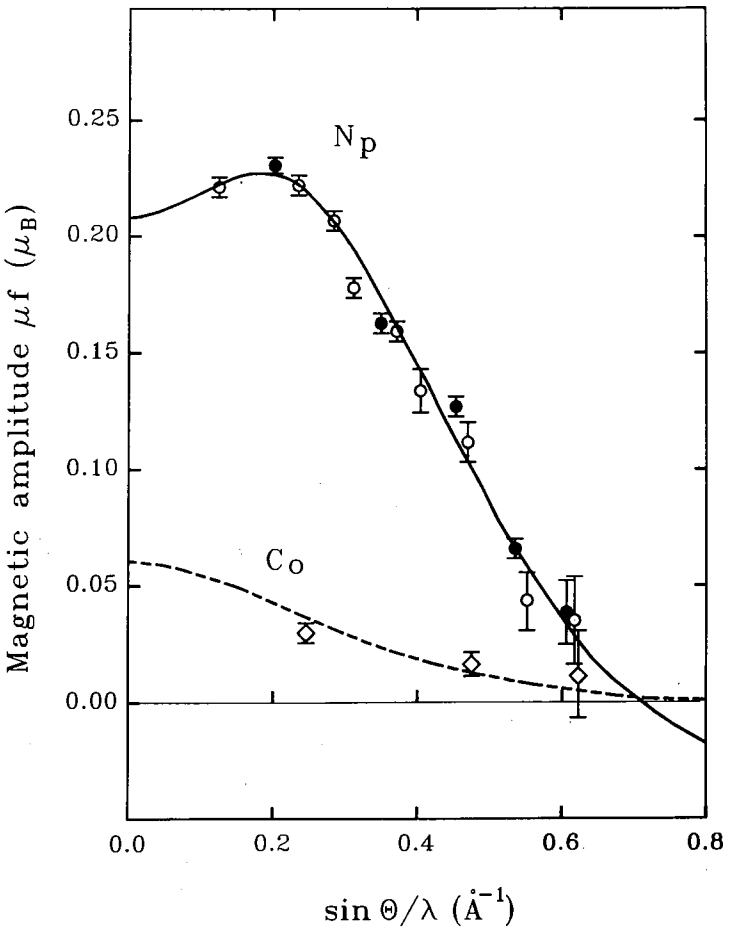

Fig. 1.5 Magnetic amplitude (μf) for Np (open and closed circles), and Co (open squares), as measured by polarized neutron diffraction in $NpCo_2$. The solid line through the Np-points is the best fit giving excellent agreement with theory

Major progress was made this year in understanding the structural changes that occur when a "charge-density wave" develops at ~ 43 K in alpha uranium. We have now found that two of the three components of the CDW exhibit "lock-in" transitions, in which the repeat unit becomes an integer number of original unit cells. Higher-order components also suggest that the modulation adopts an almost square-wave pattern. These observations are consistent with the electron microscopy patterns, in which regular lattice arrays are separated by fault regions. This work has consequences for our understanding of martensitic phase transformations in general, and for the many such transformations in actinide metals in particular.

A start was made this year on a new project aimed at measuring magnetic effects in crystals using an X-ray synchrotron source. Initial experiments have been performed at both the Daresbury and Brookhaven synchrotrons. At Brookhaven we were able to perform the experiments at the M_{IV} and M_V uranium edges (~ 3.5 keV) and have seen strong resonance effects from a single crystal of UO_2. Comparison with measurements performed on UAs show that the resonance line-widths are largely determined by atomic physics (i.e. there are no correlation effects). The technique will be most useful for heavier actinides and surface studies. A further goal is the separation of spin and orbital components.

References

[1] M.S.S.Brooks and P.J.Kelly, Phys.Rev.Lett.51 (1983) 1708
[2] M.Wulff, G.H.Lander, J.Rebizant, J.C.Spirlet, B.Lebech, C.Broholm, and P.J.Brown, Phys.Rev. B37 (1988) 5577

Theory

Theoretical studies have concentrated upon mainly the nature of spin and orbital magnetism in actinide compounds - where several predictions have been made - and upon the conditions for magnetic moment formation and further studies of cohesive properties.

The magnetic moments and magnetic form factors of Np and Pu intermetallics with Fe, Co and Ni were computed. Agreement with the experiments made so far has been excellent. Research on ternary compounds of uranium started with a study of UCoAl where the meta-magnetic transition was reproduced by a fixed spin moment calculation. The composition of the magnetic moment by site and quantum number was predicted and has subsequently been verified in recent experiments.

A theory which we have called relativistic Stoner theory has been developed and applied to a number of metals and compounds. The theory gives correctly, as shown in Tab. 1.8, whether any given compound is magnetic or non-magnetic. The relativistic extension to Stoner theory removes several anomalies - e.g the magnetism in Np metal and several Pu compounds - present in the previous theory (Tab. 1.8). The cohesive properties of rare earths and actinides have also been studied from first principles using self-consistent energy band calculations. A major result is that lawrencium is found not to be a simple sp metal but the first member of a 6d transition series.

Tab. 1.8 Experimental and theoretical volumes, magnetic moments and Stoner products (fully relativistic and scalar relativistic) for $PuFe_2$, $PuCo_2$, YRh_3, Pu(fcc) and Np(fcc). Normal multiband Stoner products are given in parenthesis.

	$PuFe_2$	$PuCo_2$	Np	Pu	YRh_3
V(exp) (Å^3)	92.9	88.8	19.2	20.0	65.0
V(theo) (Å^3)	91.0	84.5			
V(theo) (Å^3) (Scalar)	83.4	81.5			
Magn. Mom. (μ_B) (exp)	μ(Pu)=0.4 μ(Fe)=1.7	para	para	para	para
Magn. Mom. (μ_B) (theo)	μ(Fe)=1.6	para	para	para	para
Stonerproduct (nonrel)	1.7	1.3	1.2(1.2)	0.9(0.9)	0.4(0.4)
Stonerproduct (rel)	1.4	0.9	0.3	0.3	0.4

PuSe: A Highly Correlated 5f-Electron Metal

Pu chalcogenides including PuSe exhibit curious properties not well understood because of incompatibility between magnetic behaviour and lattice constants: The assumption of divalent Pu with a localized $5f^6$ configuration can explain the absence of magnetic order [1, 2] but not the small lattice parameters; on the other hand, the assumption of trivalent Pu with the $5f^5$ configuration would be more consistent with the lattice parameters but cannot explain the observed almost temperature independent magnetic susceptibility [2].

In an attempt to reconcile the contradiction, self-consistent electron-energy band calculations were performed in different ways [TUAR 86, p.118; 2]. Only within a fully relativistic treatment allowing for hybridization with other states, were the magnetic properties and the calculated lattice parameters in agreement with experiment. For this case, the Pu chalcogenides were calculated to be semiconductors with band gaps of about 0.3 eV. Consequently, these compounds were designated "Relativistic Semiconductors".

Photoemission spectroscopy permits, in a very straightforward way, the investigation of valence and conduction electron states: In the case of a semiconductor, no photoelectron emission will be observed at the Fermi energy E_F located within the band gap. To test the concept of a "Relativistic Semiconductor" 4f core level and valence band photoemission spectra, in particular high-resolution ultraviolet photoemission spectra (HRUPS), have been recorded for single crystal PuSe.

The PuSe single crystal was cleaned for several weeks by repeated cycles of annealing and argon ion sputtering until the surface was practically free of oxygen contamination. The conduction band spectra recorded by HRUPS at T = 70 K showed, just at E_F, a strong emission of major Pu-5f character as unambiguously determined from the typical photoionization cross-section variations for 5f electrons.

This preliminary result was confirmed by measurements for "in-situ" scraped PuSe surfaces. Surprisingly, the emission of Pu-5f electrons at E_F was even higher, despite the fact that the relative amount of Pu in the surface was reduced compared with the sputtered surface. Fig. 1.6. shows the conduction band spectra for scraped PuSe recorded at 70 K for different excitation energies. At low excitation energy (16.7 and 21.2 eV) the emission is dominated by broad structures between 3.5 and 6eV binding energy; they are attributed to mainly Se-4p-derived valence-band states. At higher excitation energy (40.8 eV) the sharp structures at E_F, 0.5 and 0.9 eV and a broad emission at about 2 eV binding energy are dominating, and are identified to have mainly Pu-5f character. *Thus PuSe is not a semiconductor but a metal.*

Comparison with electron-energy band calculations [3] shows that the experimentally determined Se-4p band is about 2.5 eV lower in binding energy; the calculations do not account for the broad emission around 2 eV. Since these calculations are only performed within a single electron picture, they do not include electron-electron correlation. Therefore the structure at 2 eV is attributed to a localized response of highly correlated Pu-5f electrons. The uniquely sharp and intense structures close to and at E_F are either reflecting the electron density of delocalized Pu-5f states, similar to the calculated 5f band states, or indicating extraordinarily strong Kondo resonance effects. The latter would imply that PuSe is a lightweight heavy fermion system with an unusually high Kondo temperature of about 1000 K. Both pictures are qualitatively consistent with the Pu-4f core level spectra.

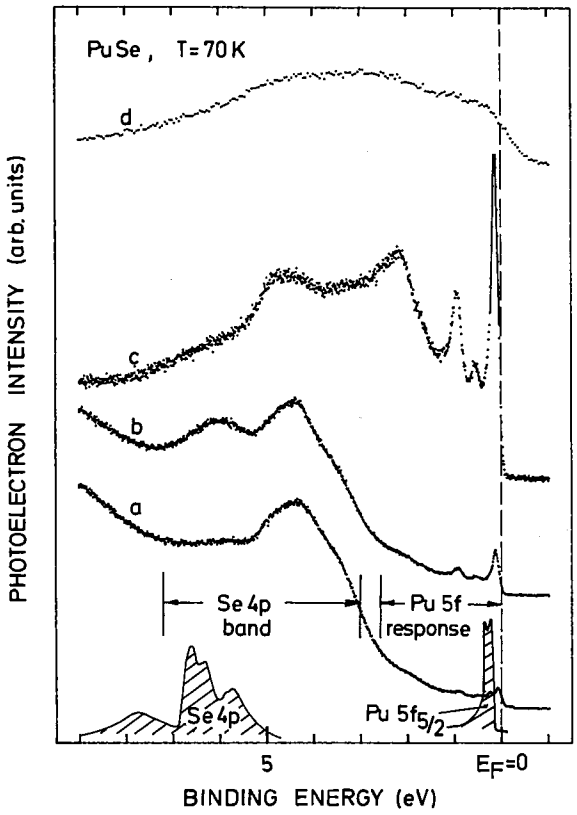

Fig. 1.6 HRUPS/XPS conduction band spectra of PuSe for a) 16.7 eV (NeI), b) 21.2 eV (HeI), c) 40.8 eV (HeII), and 1486.6 eV (MgK_α) excitation energy. The calculated density of occupied electron states [3] is displayed for comparison (hatched area)

Temperature dependent photoemission measurements of the Pu-4f core levels and the conduction band, together with quantitative calculations, may permit a clear discrimination; preliminary temperature dependent measurements show unexpectedly strong variations indicating that PuSe is a high-temperature Kondo system.

References

[1] D.J. Lam and A.T. Aldred, The Actinides: Electronic Structure and Related Properties, Vol.1, eds. A.J. Freeman and J.B. Darby, Jr., (Academic Press, New York and London, 1974), p.110
[2] G.H Lander, J. Rebizant, J.C. Spirlet, A. Delapalme, O. Vogt and K.Mattenberger, Physica 146 B (1987) 341
[3] M.S.S. Brooks, J.Magn.Magn.Mat. **63&64** (1987) 649

High-Pressure Studies on Actinide Systems

B1 Type Compounds

The general scope of the study of this family of compounds was described in TUAR-88. In 1989, plutonium monoselenide was studied up to 47 GPa, at room temperature (Fig. 1.7). The compound has been found to undergo a second-order

crystallographic phase transition around 20 GPa. This phase can be described as a distorted B1 type structure. It has rhombohedral symmetry. Then PuSe transforms to a new phase around 35 GPa, which can be indexed in the cubic CsCl-type (B2) structure. The volume collapse at this phase transition is 11 %. When releasing pressure, hysteresis to the inverse transformation was observed down to 5 GPa. From the pressure-volume relationship, the bulk modulus has been determined as $B_0 = 98$ GPa and its pressure derivative as $B_0' = 2.6$.

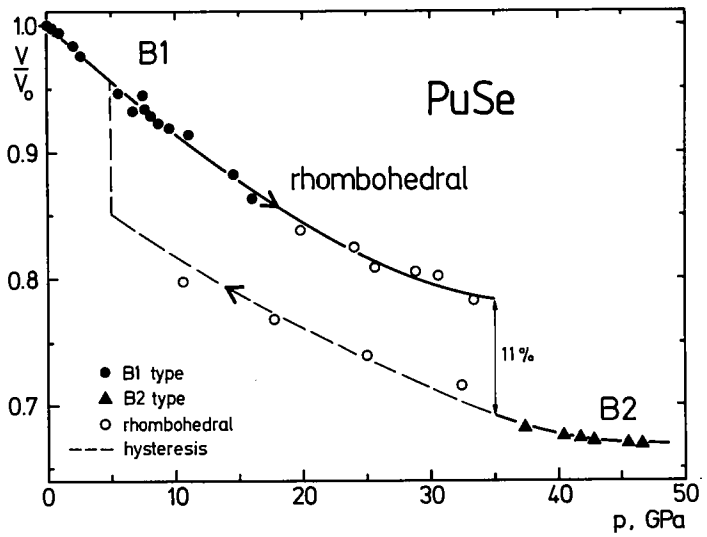

Fig. 1.7 Equation of state (relative volume vs. pressure) for PuSe. Dashed line: Measurements at decreasing pressure. Note the volume decrease of 11% at 35 GPa on in-crease of pressure

In total, 12 monopnictides and 9 monochalcogenides of the actinides Th, U, Np and Pu have been studied up to now by x-ray diffraction in our diamond anvil cells. The results obtained allow us to clearly recognize systematic trends in the nature of the high-pressure phase, the transition pressures, the pressure ranges of hysteresis, and in the compressibility.

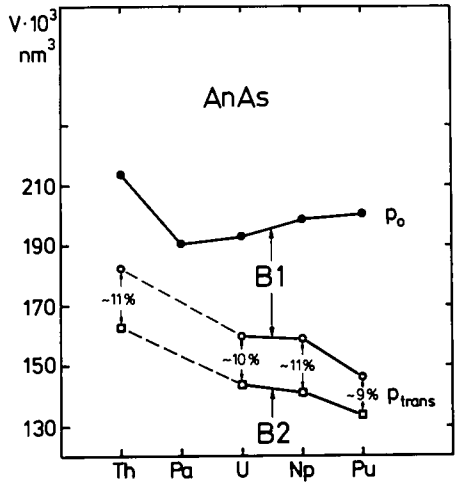

Fig. 1.8 Normalized unit cell volumes of the B1- and the B2-type phases of actinide monoarsenides at ambient pressure and near the phase transition. ● B1, ambient pressure; o B1, near the transition pressure; □ B2, near the transition pressure

As an example, Fig. 1.8 shows, that an actinide monoarsenide transforms to the B2 type at higher compression, thus at higher pressure, with increasing atomic number of the actinide.

We have recently started to include in this study solid solutions of two of the B1 type compounds. Thus, high-pressure x-ray diffraction measurements, using synchrotron radiation, have been performed on UP_xS_{1-x} (x =0.6; 0.8) up to 53 GPa. UP_xS_{1-x} forms a solid solution with a B1 (NaCl) structure. For both compositions a second order phase transition is observed around 10 GPa. The high-pressure phase can be described as a distorted B1 structure with a rhombohedral symmetry. For the compound $UP_{0.8}S_{0.2}$ a second phase transition is observed, which starts at 37 GPa and is complete at 46 GPa. This high-pressure phase seems to have orthorhombic symmetry. It has some similarities to the high pressure phase of UP [1] ,although the intensities do not fit for all reflections. $UP_{0.6}S_{0.4}$ shows only some small indications for a phase transition at the highest attained pressure (53.5 GPa). In conclusion we observe that the phase transition in UP shifts to higher pressure, when phosphorus is replaced by sulfur. The bulk modulus B_0 and its pressure derivative B_0' have been determined.

Actinide Dioxides

Former high-pressure studies of UO_2 [2] and NpO [3] have recently been extended to the dioxides ThO_2 and PuO_2. The observed high-pressure phases of ThO_2 and PuO_2 both exhibit similar diffraction spectra. ThO_2 undergoes a phase transformation at 40 GPa. This high-pressure phase is stable up to 55 GPa, highest pressure reached in the experiment. In the case of PuO_2 we were unable to determine the pressure at which the structure changes, due to the deep red colour of this compound under pressure which interferes with the red fluorescence line of ruby used for pressure determination.

The high-pressure phases resemble orthorhombic high-pressure phases observed for other fluorite type dioxides such as NpO_2[3], UO_2[2] and CeO_2[4]. Indexing is under way.

Actinide and Lanthanide Metals

Within this group of materials, the accent is now on the study of binary alloys between neighbouring actinides. The results of these studies will refine the general diagram of the phase relations of actinide metals under pressure (see TUAR-86, pp. 115 - 117). First results for the δ phase in the U-Np system are presented here. On the other hand, lanthanides are a necessary reference in actinide studies. It is in this sense that we have undertaken the HPXRD study of Pm, the only lanthanide that, because of its high β-activity, had not yet been studied by this method.

High-pressure x-ray diffraction study of the delta phase in the uranium-neptunium binary system

High-pressure x-ray diffraction studies were performed on a uranium-neptunium binary alloy ($U_{0.4}Np_{0.6}$) at room temperature up to 62 GPa. At room temperature and ambient pressure the alloy is a simple cubic phase with 58 atoms per unit cell. Its lattice parameter, a = 1063,5 (5) pm, was accurately determined on a powder diffractometer. When increasing pressure up to 62 GPa (highest pressure reached in this experiment), no phase transition was observed. However, the relative vol-

ume (V/V_0) compression curve shows that a discontinuity in the compressibility is likely to occur at about 20 GPa.

The bulk modulus and its pressure derivative were determined, by fitting the V(p) data to the Murnaghan equation. According to the pressure range used to fit the V(p) data, the following values were obtained:

$0 < p < 20$:	$B_0 = 82$ GPa	$B_0' = 9$
$0 < p < 62$:	$B_0 = 93$ GPa	$B_0' = 8$

Promethium metal

We have studied Pm-147 (element 61) metal under pressure. Its behaviour under pressure provides another important piece in the puzzle of changes in bonding and structure of the f-elements under pressure, as a function of their f-electron occupancy and position in each of the two series. The study of Pm metal was targeted because of the pivotal position of this element in the 4f series. There is evidence that under pressure (43 GPa) the 4f electrons of Nd (element 60) delocalize while those of Sm (element 62) do not delocalize up to 100 GPa.

We observed that two phase transitions occur by 18 GPa. The first transition, which occurred in the region of 10 GPa, was from its room temperature/pressure dhcp form to an fcc form (Fm3m space group). The second was the conversion of this fcc form at 18 GPa to a third form, that has been frequently referred to as a distorted fcc structure in other studies with the lanthanide and transplutonium elements. The latter structure was retained up to at least 40 GPa. Above 40 GPa, subtle changes in the X-ray spectra were noted and the fit of the data to the distorted fcc structure became more difficult. These conditions suggested the onset of an additional structural change, although direct evidence for such a change was not obtained at 60 GPa. From these studies of Pm metal, a bulk modulus of 38 GPa was derived for it.

Although we did not obtain evidence for the delocalization of the 4f electrons of Pm up to 60 GPa (e.g., formation of the alpha uranium-type structure), it should be noted that the pressure and phase sequences of Pm metal parallel those of Nd, Am, and Cf metals prior to the partial delocalization of their f-electrons.

References

[1] J. Staun Olsen, L. Gerward, U. Benedict, S. Dabos, O. Vogt Physical Review **B 37** (1988) 8713

[2] U. Benedict, S. Dabos, C. Dufour, J.-C. Spirlet, M. Pagès, J. Less-Common Met. **121** (1986) 461-468

[3] S.J. Duclos, Y.K. Vohra, A.L. Ruoff, A. Jayaraman, G.P. EspinosaPhysical Review **B 38** (1988) 7755-7758

[4] U.Benedict, G.D. Andreetti, J.M. Fournier, A. Waintal, J. Phys. Lett. **43** (1982) L171-L177

Materials Research on Actinide Systems

Preparation of Metallic Glasses and Microcrystalline Materials

Splat cooling equipments using levitation and arc melting were built up and tested. Metallic glasses of magnetic materials, $UFe_{14}B$, $UFe_{14}C$, were prepared and characterized by x-ray and electron diffraction. The magnetic properties are under investigation. In search for new materials with heavy fermion behaviour attempts to prepare new ternary compounds are underway. Splat cooled samples of URu_2Si_2, URu_2Ge_2, UMo_2Si_2, $ThMo_2Ge_2$, UAg_2Si_2, UAg_2Ge_2, $ThAg_2Si_2$, $ThAg_2Ge_2$ were prepared. The characterization of the samples by x-ray diffraction is in progress.

Collaborative Actinide Research

The Institute also produces many materials that are of principal interest to our outside collaborators, although frequently the same material is examined both in-house as well as with other physical techniques available to collaborators.

Some examples of this are:

(1) The use of the Mössbauer technique to study $NpRh_2Si_2$, NpSb, and $NpCo_2$ at CNRS Strasbourg, and $NpSn_3$ at high pressures at the Technical University of Munich;

(2) An examination of the magnetic transition temperatures as a function of time and isotope content on $^{239}PuSb$ at AERE, UK. Since a sample of $^{242}PuSb$ was also available the measurememnts could be normalised to zero radiation damage, as this is the case for ^{242}Pu;

(3) Low temperature resistivity measurements have been completed on single crystals of all the plutonium monochalcogenides at CEN Grenoble. The resistivity of all three compounds *increases* as the temperature decreases (the opposite is expected of a metal), and from Hall effect measurements the authors suggest these materials to be small-gap semiconductors;

(4) In a collaboration between ETH Zürich and CEN Grenoble magnetisation and neutron diffraction experiments have been performed on mixed NpSb-NpTe single crystals. NpSb is antiferromagnetic, but with the replacement of Sb by ~5% Te, the material develops a ferromagnetic component. This can be deduced from the results of the magnetisation experiments, but is seen directly in the neutron scattering experiments. Fig. 1.9 gives the intensity of the (111) reflection, which shows the ferromagnetic component appearing at $T_c = 143$ K, and the (001) reflection which indicates that a commensurate type-I form of antiferromagnetic modulation appears at $T_c = 89$ K. This is an unusual combination of components. For NpTe-concentrations of 10 and 15% the compositions are ferromagnetic. Work is in progress on higher concentrations. It is of particular interest that NpTe is a complex antiferromagnet and *not* a ferromagnet, as is the case of the analogous uranium compounds.

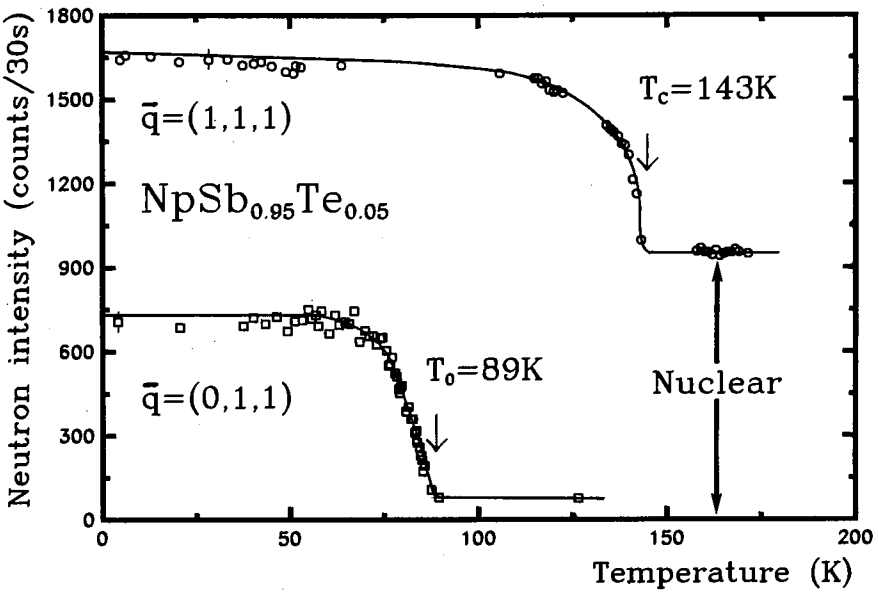

Fig. 1.9 Magnetic Bragg intensities of $NpSb_{0.95}Te_{0.05}$ as a function of temperature. The peak (111) represents the ferromagnetic component and the superlattice peak (011) the AF type I component

1.2 Exploratory Research

Acoustic Aerosol Scavenging

Introduction

In the project 'Acoustic Aerosol Scavenging' the feasibility of the use of high intensity acoustic waves to combat airborne spreading of accidentally released radioactive or toxic material is being investigated. The potential areas of application range from small scale laboratory spills and fires to major releases of hazardous material into the atmosphere. During the reporting period, the acoustic agglomeration of submicron combustion aerosol produced by burning rubber in a 15 m^3 chamber was studied and compared to the earlier results in a 4.5 m^3 chamber. Of particular interest in these laboratory scale experiments is the rate of decrease of the mass loading, the growth rate of particles, and how these scale with acoustic power at a source frequency of 21 kHz.

The basic mechanism behind acoustic agglomeration of aerosols has been described in earlier reports in detail [1]. It is sufficient to state here that by applying high intensity sound waves to particles in a gas the particle collision rates can be increased by orders of magnitude. The resulting collisions lead to agglomeration of the particles under the action of short range surface forces.

Experimental

Piezoelectric transducers rated at 400W electrical power and 75 % efficiency were used in these experiments. Three identical 21 kHz transducers were available and were used both singly in a 4.5 m^3 chamber and as 1200 W array in a 15 m^3 chamber. The emitting surface of the transducer was a titanium plate 48 cm in diameter. The surface of this plate was specially profiled to counteract radial flexing of the emitting surface that would otherwise prevent propagation of a plane wave [2].

The test aerosol was generated by burning rubber in the chamber for about 5 mins. This smoke aerosol met the requirements of high mass loading (1 gm^{-3}) and small particle size (0.1 - 1 μm).

Chambers of 4.5 and 15 m^3 were used and the transducers were mounted facing the side walls. A single 400 W transducer was used in the 4.5 m^3 chamber and a horizontal array of 3 transducers was used in the 15 m^3 chamber. No attempt was made to optimize the distance between the transducer and wall to ensure a standing wave: the whole chamber acted as a resonant cavity.

Sound pressure levels were measured using a B&K microphone. Measurements were made at different positions within the chambers and the quoted values represent average values. The signal observed on an oscilloscope was not a pure sine wave but no attempt was made to analyze the higher harmonics. The true sound pressure level was probably higher than the values quoted here: 149 dB max. in the 4.5 m^3 and 143 dB max. in 15 m^3 chambers respectively.

The aerosol agglomeration rate was measured in two ways. The first was to determine the mass loading of the aerosol by weighing filter samples. Mass loading data excludes material levitated in the sound field. The change in mass

loading with time is thus a record of the mass of those aerosol particles with an aerodynamic diameter low enough to remain in aerosol suspension.l

The second method was to measure the size of the suspended aerosol particles and agglomerates using a Galai CIS-1 particle size analyser with a range of 0.5 - 600 micrometers. Samples for this measurement were taken by exposing glass microscope slides in the chamber for a few seconds. These slides were then analysed in a scanning laser beam to establish the geometric size distribution of particles. The same samples were also analysed by image analysis [3].

Results

Mass loading measurements were also made with an array of 3 x 400 W transducers in a 15 m^3 chamber i.e. a scale up of a factor of 3 in both volume and power over previous experiments. The results were very similar to those obtained with a single 400 W transducer in a 4.5 m^3 (Fig. 1.10) demonstrating that a scale up is possible.

In the absence of ultrasound the volume median diameter of soot agglomerates was measured to increase from an initial value of 10 to 70 μm in about 15 mins. In contrast, with the array of 3 x 400 W transducers the same increase was obtained in about 10 s (Fig. 1.11).

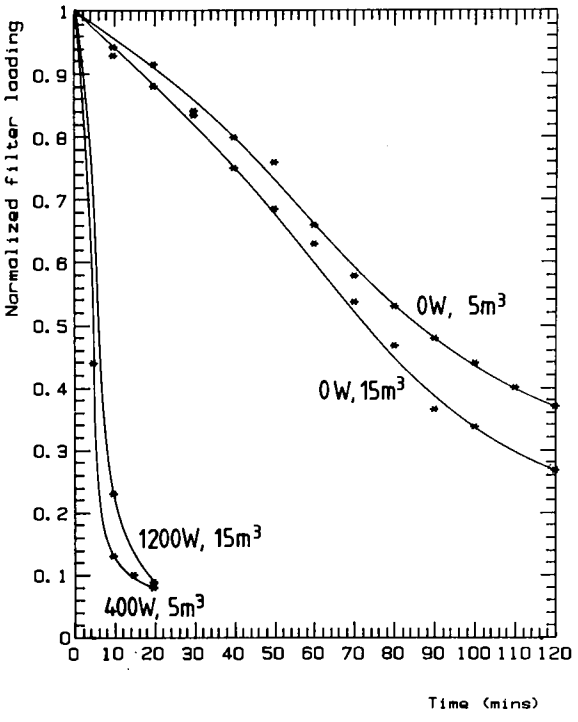

Fig.1.10 Decrease in mass loading in experiments differening in scale by a factor of 3.

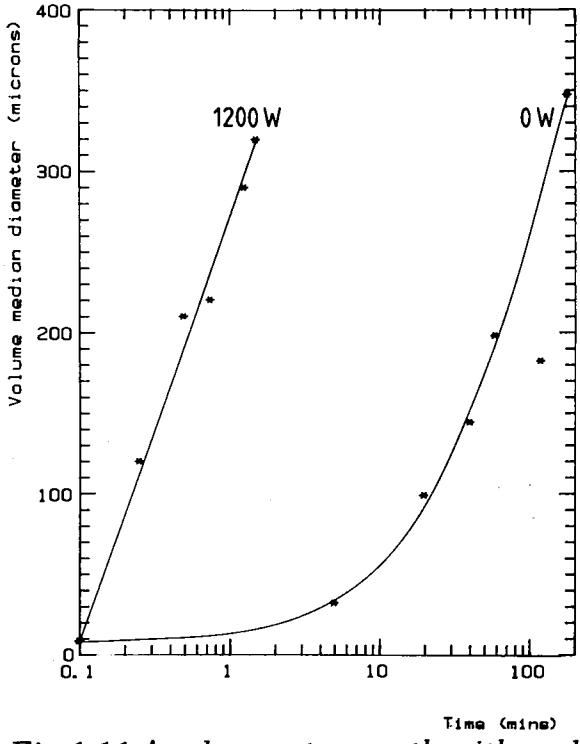

Fig.1.11 Agglomerate growth with and without a sound field

Scanning electron microscope pictures of soot agglomerates formed in an acoustic field (Fig. 1.12 b) show an open agglomerate structure that is nevertheless significantly more compact than the classic "chain agglomerate" structure of agglomerates formed by Brownian motion (Fig. 1.12 a). Acoustically formed agglomerates are thus denser and will have a somewhat greater sedimentation velocity than Brownian agglomerates of the same dimensions. Large agglomerates that levitate in the sound field are very thin "two-dimensional"

flakes of soot. The aerodynamic diameter of such 1 cm diameter soot flakes was measured by sedimentation to be about 50 µm.

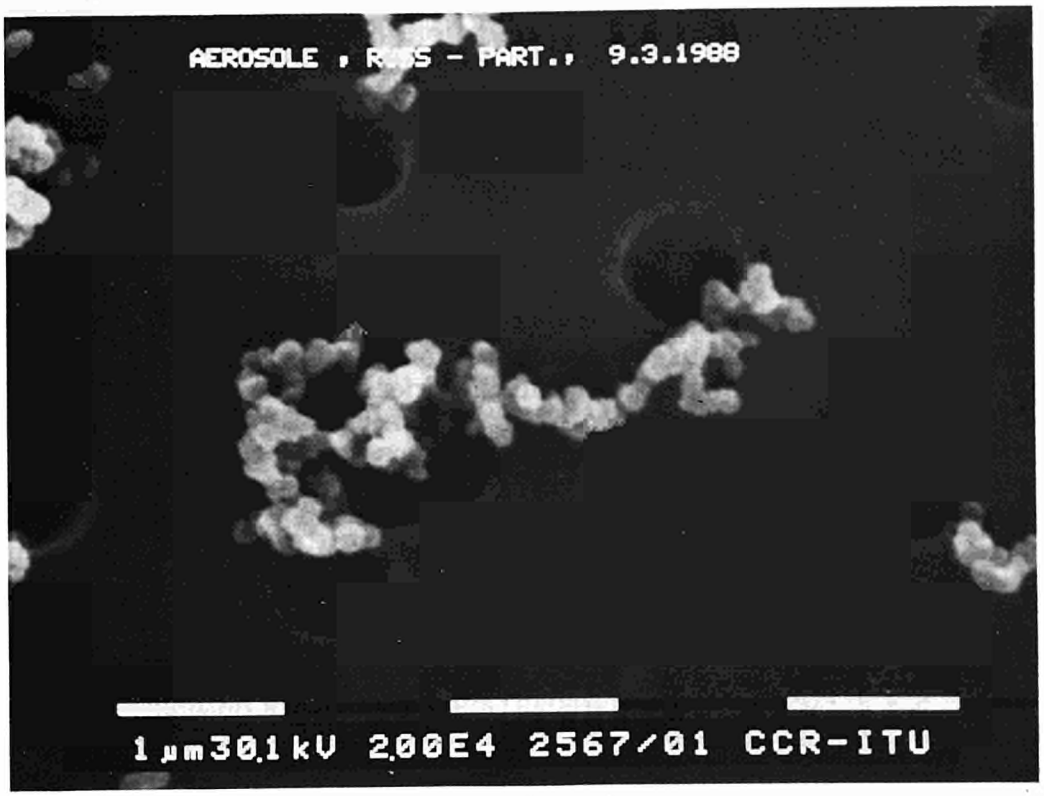

a)

b)

Fig. 1.12 Agglomerates a) before and b) after acoustic treatment

Discussion and Conclusions

The relatively long aerosol generation phase (5 mins) in the static chamber used in these experiments, resulted in agglomeration by Brownian motion to sizes of 10 μm before switching on the sound field. For better control of parameters during the initial stages of agglomeration a dynamic system would be more appropriate, i.e. continuous generation of aerosol and flow through the acoustic chamber to obtain a well defined residence time in the field. Such experiments under dynamic conditions are planned and will be carried out during the next reporting period.

Nevertheless, the results for the median volume diameter show that acoustic treatment of a dense smoke aerosol at high sound pressure levels increases the agglomeration rate by several orders of magnitude. However, because the smoke agglomerates are open structures rather than compact spheres, their aerodynamic diameter, and hence sedimentation velocity, increases only slightly even for a large increase in volume. Thus, despite the rapid increase in agglomerate size, the low sedimentation velocity of the agglomerates results in a relatively slow decrease in mass loading in the chamber. In contrast, an aerosol of liquid droplets would coalesce to form spherical droplets with much higher sedimentation velocities and a correspondingly rapid decrease in mass loading would be expected.

Future experiments will concentrate on acoustic agglomeration of well defined aerosols under dynamic flow conditions. A potential industrial application here is the acoustic pretreatment of fine particles in gas streams to increase particle sizes. Agglomerates can then be removed efficiently using e.g. electrostatic filters or cyclones.

In addition agglomeration experiments, under static and dynamic flow conditions, are foreseen using seed aerosols (initially water droplets). Based on the results presented here, successful agglomeration of soot particles to water droplets should result in a much reduced 'clearing time' of the chambers; a result of significant importance both to industrial application in 'open-air' applications [4].

References

[1] TUAR 1987 p. 183 - 196, TUAR 1988 p. 191 - 198

[2] J.A. Gallego-Juarez, G. Rodriguez-Corral, L. Gaete-Garreton"Ultrasonics" 16 (1978) 267-271

[3] J. Magill, S. Pickering, S. Fourcaudot, J.A. Gallego-Juarez, E. Riera-Franco De Sarabia, G. Rodriguez-Corral "Ultrasonics" (1989), to be published

[4] J. Magill, "Ultrasonics" (1989), to be published

1.3 S/T-Support to Community Policies

1.3.1 Analytical Support to the EURATOM Safeguards Directorate

Part of the continual support to the European Commission consists of the analysis of Safeguards samples collected and sent by the Nuclear Inspectorate, Luxembourg. The results and comparison with declared values cannot however, be published for reasons of confidentiality. 2 man-years are specified for development, and the status of this work is briefly reported here.

As part of the on-line evaluation of data, an expert system [1] has been further developed and extended to include an automatic titration device.

This apparatus (an automatic titrator, type RADIOMETER) is being connected to the central PDP-11 computer system. Connections are made to the titrator console, the balance used for dispensing and aliquoting the samples, and a printer. A visual display unit allows the operator to start the program(s) and to keep an overview, on-line, of the data already collected held in the form of a databank.

The titration requests will be generated by the expert system which causes the bar-code labels for the sample containers (dissolution, dilution, weighing and titration) to be printed and determines the sample and details of the aliquotation for the titrator operator. The labels have the DCS analysis number printed plus an internal laboratory bar-code which is checked at each critical step of the analysis.

Already planned (and software partly written) is the connection of a K-edge apparatus to the central computer. The transmission of data occurs block by block with checksum surety, following the format already used for transmissions to the central computer from the PC-AT with the expert system and from the mass-spectrometers.

The second development activity concerns the analysis of solid residues in HAW or input solutions. At present these analyses are being made using destructive techniques but a future method of analysis to be utilised is by ICP/MS employing the technique of laser ablation directly on the solid material.

The third activity concerns the development of an on-site laboratory to be situated at a processing plant and capable of analysing the input and output of the plant for Safeguards. This work is at the stage that a conceptual report is being prepared but the main parts of the concept are already clear and involve the extensive use of laboratory robots to prepare the samples for measurement, the use of a central computer to control and communicate with the measuring apparatus and the robots and also with the Institute in Karlsruhe.

The flow of the measurements and the necessary checking will be controlled from the Institute. This will involve not only the statistical supervision of the measured results but also the initiation of standards which will be inserted into the measurement stream.

Reference

[1] D. Wojnowski, B. Brandalise, M. Merten, L. Koch, 'Expert System for Preparation of Safeguards Sample Analysis', 11th Symposium on Safeguards and Nuclear Material Management, Luxembourg, 30 May - 1 June, 1989

1.3.2 Evaluation and Automation of Analytical Techniques

Four tasks are currently being carried out in the frame of the EURATOM/IAEA support programme:

- Task MT9: Software for quality control of analytical results on input samples.

The scope of an expert system to carry this out has already been defined. It will incorporate isotope correlation techniques based on a databank of pertinent measured data and also the measurement source errors.
The software will be based on that already written for and in use by the Luxembourg Safeguard Inspectorate but extended to include the quality control indicated above.

- Task MT14: the rationalisation of analytical work, particularly in respect to reprocessing plant samples.

The field testing of a K-edge densitometer is still in progress and has been extended to analyse filter samples and to the determination of solution densities before analysis.

- Task MT14A: the automatic conditioning of samples by robots.

A glove-box containing a laboratory robot for the conditioning of input samples to prepare them for mass-spectrometry measurements has been constructed for the IAEA and delivered in July 1989. The instruction manual has been written and will shortly be delivered. A joint evaluation and exchange of experience made with the robot will be made shortly.

- Task MT14B: Cooperative field test of on-site sample conditioning by robots.

It is proposed to test the robot system developed above in MT14A in-field. The IAEA has defined the pilot plant at Gatchina near Leningrad as a site where the testing can be carried out. The scope of the experiment and the design of the robot are at present under discussion.

1.4 Work upon Request

1.4.1 Fabrication of Plutonium Dioxide Sol-Gel Spheres (DARM-Project JRC Geel)

On request of CBNM, JRC Geel PuO_2 spheres with different isotopic compositions are prepared as reference material for destructive mass-spectrometry (DARM-Project) by Sol-Gel technique. During test runs problems with respect to mechanical stability and breakage of the spheres occured. In order to understand and solve these problems an investigation of the different process steps was started.

In the last Annual Report the influence of the concentration of Pu on the autoreduction process was discussed (TUAR 88, 120).
In parallel to the investigation on the autoreduction further experiments have been carried out for reduction of Pu(VI) to Pu(IV) with H_2O_2 as reductant and formation of polymeric Pu-solution.
To achieve an appropriate polymeric Pu-solution one must link the reduction and polymerisation processes together. In this step the adjustment of the acidity which is made with ammonia solution plays an important role. To produce the Pu(IV)-species the reduction must be executed in an acidity range between 0.1 and 0.05 in HNO_3, the favourable condition for polymerisation, a range where no Pu(III) occurs [1]. This procedure results in a polymeric Pu-solution with an average content of about 1 to 1.5 moles Pu-solution. This process step is reproducible and a reliable control by spectrometric measurement is available. In Fig. 1.13 typical spectra are shown.

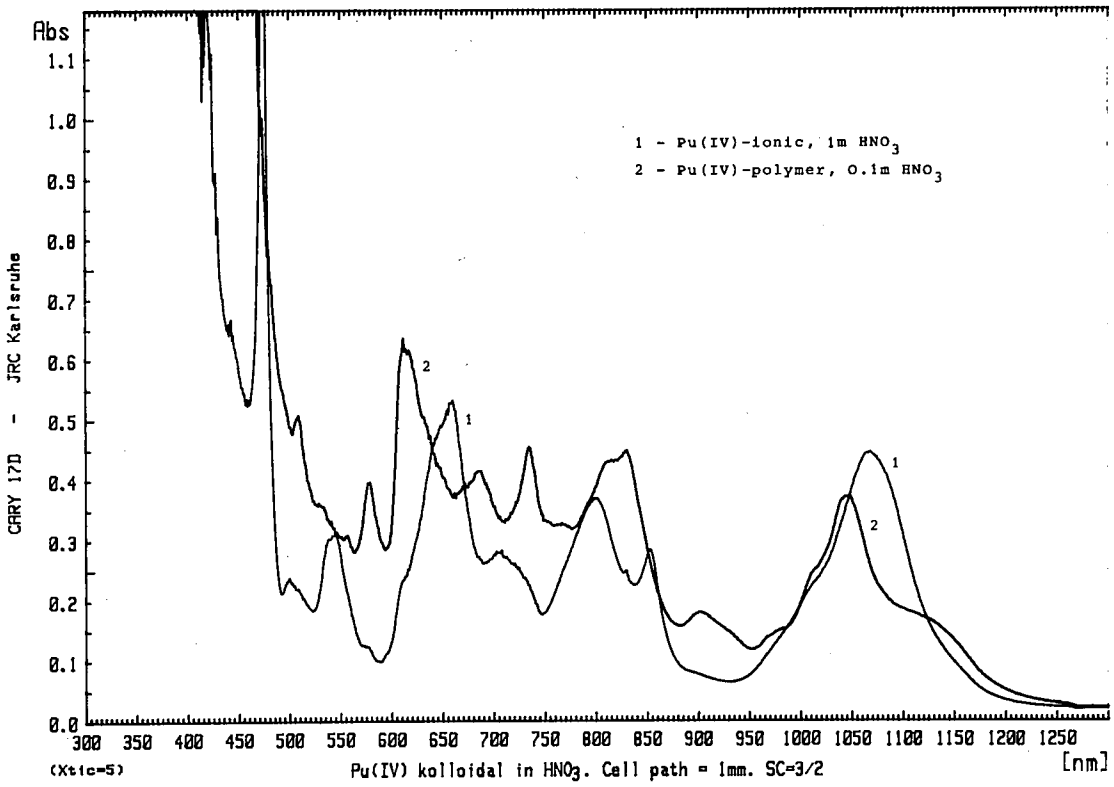

Fig. 1.13 Absorption spectrum 1 is from a Pu(IV)-ionic solution, whereas spectrum 2 is for a Pu(IV)-polymeric

During calcination breakage of spheres occured. An exothermic reaction during the precalcination step - 400 °C, Air - was observed. This reaction starts at 200 °C and could be explained by a catalytical decomposition of Methocel, caused by traces of NH_4NO_3 remained from washing,
In this first step of calcination the spheres lose about 25 to 30 % of their weight and the initial carbon content of 3 $w/_o$ drops to 0.1 $w/_o$.

At the same time gaseous decomposition products, mainly CO_2 have been measured. This indicates, that the precalcination step plays an important role and is probably responsible for the named problems. Further investigations are necessary.

Sol-Gel particles of PuO_2 with an Pu-239 content of 98,22 $w/_o$ were prepared by application of GSP-Process [2]. 60g PuO_2 spheres are ready for shipping to CBNM, JRC Geel. The typical shape of the spheres is shown in Fig. 1.14.

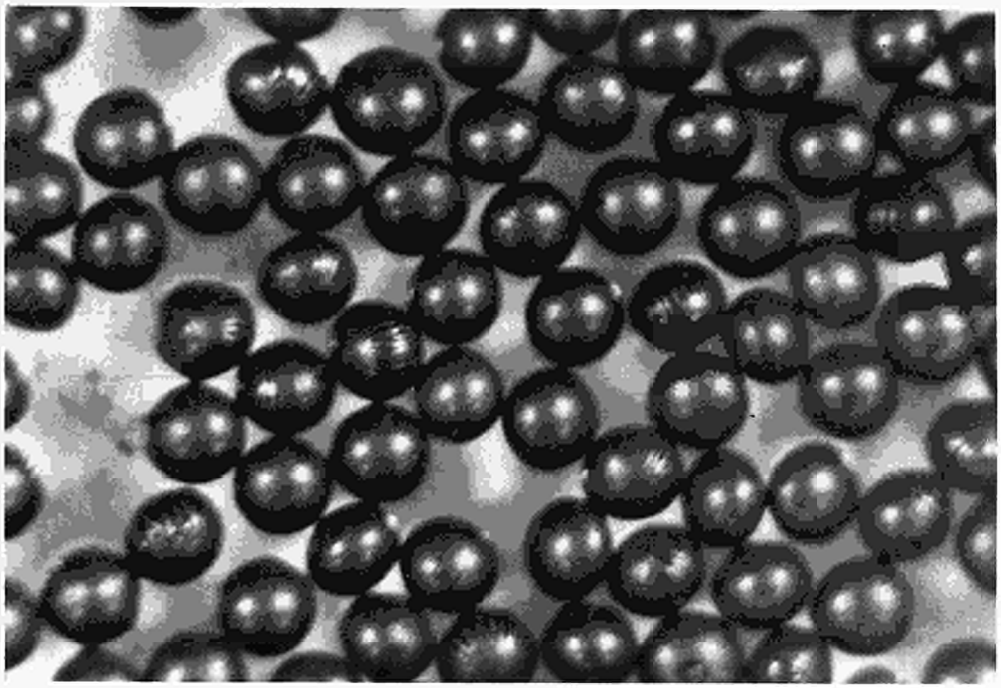

Fig. 1.14 Plutonium dioxide spheres after calcination at 800°C in air

References

[1] H.G. Schneider, TU - Technischer Bericht 88/1, 1980

[2] G. Brambilla, A. Facchini, P. Gerontopoulos, D. Neri, "The SNAM-Process for the Production of Ceramic Nuclear Fuel Microspheres Symposium of Sol-Gel processes and reactor fuel cycles", Gatlinburg, Tennessee, 191 (4-7 May 1970)

1.4.2 Preparation of Reference Standards for K-edge - X-ray Fluorescence Spectrometry

An agreement was concluded between DCS Luxembourg and ITU (see TUAR 88, p. 183), in order to make on-line measurements of the Pu- and U-concentrations of feed solutions obtained during working steps in the reprocessing centre at La Hague, France. The preferred method is K-edge - XRF spectrometry.

This measurement method has been developed in collaboration with the Institut für Kernphysik of KfK (see TUAR 88, p. 184).
(U, Pu)-standards were necessary for the calibration of the spectrometer and were fabricated at ITU. The standards (see Fig. 1.15) are of two types:

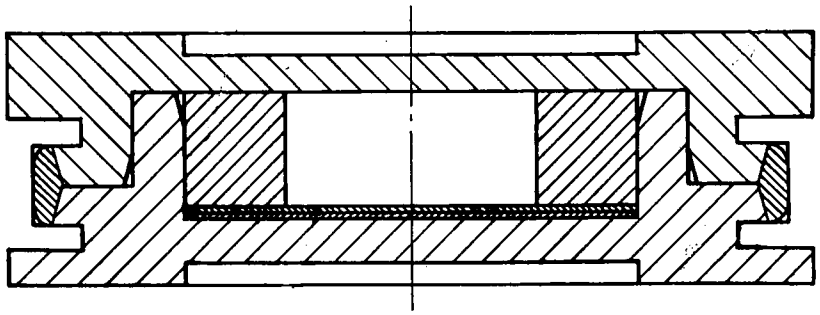

Fig. 1.15 Sample holder for U- and U,Pu-standards for K-edge XRF measurements

- U-standard, containing two discs of depleted uranium metal. The discs were stamped out of a U-foil of 1.4 mm thickness.

- (U, Pu)-standard, containing a (U, Pu)O_2 pellet, with an U/U + Pu ratio of 5 %. The fissile composition is Pu-239 = 98.2 $w/_0$ and Pu-241 = 0.08 $w/_0$. The (U, Pu)O_2 powder was prepared by coprecipitation. After calcination in air and subsequent reduction under Ar-H_2, the powder was pressed into pellets and sintered under Ar-H_2.

The standards were located into stainless steel (1.4301) capsules and sealed in glove-boxes. The welding was performed by TIG under Helium. The usual final controls (tightness, radiography, contamination) have been performed.

1.4.3 Summary of Contract Work

In 1989, the following subjects were studied in the framework of contracts with partners from industry and national institutions against payment:

- Storage and purification of enriched UO_2
- Oxidation of mixed carbide fuel samples
- Oxygen potential measurements on irradiated fuel samples
- Minor actinide alloy preparation and investigation
- Post irradiation examination of MOX fuel
- Preparation of radionuclides for therapeutical applications

Contracts under negociation dealt with

- Preparation and testing of radionuclides
- Post-irradiation examination of high burn-up fuel
- Dissolution behaviour of irradiated fuel in nitric acid
- Irradiation experiments with minor actinide fuel samples
- Boron analysis
- Electron microscopy of fuel samples

2. Human Resources

2.1 Institute's Staff

The evolution of the staff situation is given for three reference dates on the table below:

Date	A2-A4	A5-A8	B	C	D	total
01.01.	18	22	73	72	1	186
20.10.	17	22	77	74	1	191
31.12.	17	23	82	74	1	197

2.2 Visiting Scientists and Scientific Fellows

4 visiting scientists, 4 seconded experts (see below), and 12 graduate sectorial grantees from the following countries spent in 1989 prolonged periods at the Institute:

B (3)	I (1)
F (8)	P (1)
D (3)	UK (1)
GR (2)	non-EC (2)

2.3 Secondment from other laboratories

4 experts were delegated from other European research establishments to carry out specific tasks at the ITU in 1989, i.e. from CEA-CEN Grenoble (F), CEA-CEN Cadarache (F), EDF (F), and from the University of Liège (B).

Annex A: List of Publications

1. Scientific and Technical Articles

(s : submitted)

M. Thomas, Hj. Matzke
Sodium Diffusion in the Nuclear Waste Glass GP 98/12
J. Am. Cer. Soc. **72** (1989) 146-147

U. Benedict
General Diagram of the Phase Relations of Actinide Metals under Pressure
High Pressure Research 1 (1989) 139-147

L. Gerward, J. Staun Olsen, U. Benedict, S. Dabos
H. Luo, J.-P. Itié, O. Vogt
Bulk moduli and high-pressure phases of the uranium rocksalt structure compounds: I. The monochalcogenides
High Pressure Research 1 (1989) 235-251

J. Staun Olsen, L. Gerward, U. Benedict, S. Dabos
J.P. Itié
Bulk moduli and high-pressure phases of the uranium rocksalt structure compounds: II. The monopnictides
High Pressure Research 1 (1989) 253-266

J.-P. Schoebrechts, R. Gens, J. Fuger, L.R. Morss
Thermochemical and Structural Studies of Complex Actinide Chlorides $Cs_2NaAnCl_6$(An = U-Cf); Ionization Potentials andHydration Enthalpies of An^{3+}-Ions
Thermochim. Acta **139** (1989) 49-66

J. Staun Olsen, L. Gerward, U. Benedict, H. Luo
Crystal Structure and the Equation of State of ThoriumMonophosphide for Pressures up to 50 GPa
J. Appl. Crytallogr. **22** (1989) 61-63

M. Wulff, G.H. Lander, B. Lebech, A. Delapalme
The Cancellation of Orbital and Spin Magnetism in UFe_2
Phys. Rev. **B 39** (1989) 4719-4721

G.H. Lander, J. Fuger
Actinides: The Unusual World of the 5f Electrons
Endeavour **13,** No. 1 (1989) 8-14

S. Dabos-Seignon, U. Benedict, J.C. Spirlet, M. Pagès
Compression Studies on PuAs up to 45 GPa
J. Less-Common Met. **153** (1989) 133-141

M.R. Spirlet, J. Rebizant, C. Apostolidis, G.D. AndreettiB. Kanellakopulos
Structure of Tricyclopentadienyl Uranium Bromide
Acta Crystallogr. **C 45** (1989) 739-741

J. Charlier, E. Merciny, J. Fuger
Etude de la complexation des lanthanides trivalents par l'isomère trans-1,3 de l'acide cyclopentanediamino-tetraacétique
Anal. Chim. Acta **220** (1989) 187-194

Hj. Matzke
"Nuclear Techniques in Surface Studies of Ceramics"
In Non-Stoichiometric Compounds, Surfaces, Grain Boundaries and Structural Defects
Eds. J. Nowotny and W. Weppner, Kluwer Acad. Press (1989) 321-336

E. Drosselmeyer, H.-L. Müller, S. Pickering
An Interspecies Comparison of the Lung Clearance of Inhaled Monodisperse Cobalt Oxide Particles - Part VII: Lung Clearanceof Inhalted Cobalt Oxide Particles in Sprague-Dawley Rats
J. Aerosol Sci. **20** (1989) 257-260

M.R. Bailey, W.G. Kreyling et al., S. Pickering et al.
An Interspecies Comparison of the Lung Clearance of Inhaled Monodisperse Cobalt Oxide Particles - Part I: Objectives and Summary of Results
J. Aerosol Sci. **20** (1989) 169-188

C. Ronchi, C. Syros, J. Sakellaridis
Analytical Solution of the Radioactive Volatile FissionProduct Release Equation in the Presence of Precipitationand Re-Solution
J. Nucl. Mater. **168** (1989) 65-69

O. Eriksson, B. Johansson, M.S.S. Brooks, H.L. Skriver
Electronic Structure, Cohesive, and Magnetic Properties of the Actinide-Iridium Laves Phases
Phys. Rev. **B 39** (1989) 5647-5654

H.L. Müller, E. Drosselmeyer, G. Hotz, A. Seidel
H. Thiele, S. Pickering
Behaviour of Spherical and Irregular $(U,Pu)O_2$ Particles After Inhalation or Intratracheal Instillation in Rat Lung and During in Vitro Culture with Bovine Alveolar Macrophages
Int. J. Radiat. Biol. **55** (1989) 829-842

N. Bila, E. Merciny, J. Fuger
Détermination des constantes de stabilité des complexesdes lanthanides trivalents avec les macrocycles polyaza-polycarboxyliques
Anal. Chim. Acta **221** (1989) 325-336

G. van Goethem, K. Lassmann
The Coupling Algorithm between Fuel Pin and Coolant
Channel in the European Accident Code EAC-2
Nucl. Eng. Des. **113** (1989) 323-336

O. Eriksson, B. Johansson, M.S.S. Brooks, H.L. Skriver,J. Sjöström
Itinerant Magnetism in $CeRh_3B_2$
Phys.Rev. **B40** (1989) 5270-5273

O. Eriksson, B. Johansson, M.S.S. Brooks
Metamagnetism in UCoAl
J. Phys.: Condens. Matter 1 (1989) 4005-4011

O. Eriksson, M.S.S. Brooks, B. Johansson
Relativistic Stoner Theory Applied to $PuSn_3$
Phys. Rev. **B 39** (1989)13115

M.S.S.Brooks, O.Eriksson, B.Johansson
3d-5d Band Magnetism in Rare Earth Transition Metal Intermetallics : $LuFe_2$
J.Phys.Condens. Matter 1 (1989) 5861-5874

P.Burlet, S.Quezel, J.Rossat-Mignod, J.C.Spirlet, J.Rebizant, O.Vogt
Neutron Scattering Studies of Neptunium and Plutonium Compounds
Physica B 159, (1989) 129

K. Lassmann, C. Ronchi, M. Coquerelle, C.T. Walker, M. Mogensen
The D-COM Blind Problem on Fission Gas Release: The Predictions of the TRANSURANUS Codes
Nucl. Eng. Des. (s)

J. Fuger
Effects of Ionizing Radiation
Gmelin Handbook on Inorganic Chemistry
Thorium, Supplement A 4, Chapter 4, (1989) 191-198

J. Fuger
Chemical Thermodynamic Properties - Selected Values
Gmelin Handbook on Inorganic Chemistry
Thorium, Supplement A 4, Chapter 3, (1989) 175-190

Hj. Matzke, B.W. Seatonberry, I.L.F. Ray, H. Thiele, H. Trisoglio, C.T. Walker, T.J. White
The Incorporation of Transuranic Elements in Titanate Nuclear Waste Ceramics
J. Amer. Ceram. Soc. (s)

Hj. Matzke
Surface Diffusion and Surface Energies of Ceramics.
In: Surfaces and Interfaces of Ceramic Materials
Eds. L.C. Dufour and J. Nowotny, Kluwer Acad. Publ. Netherlands (1989) 241-272

H. Blank
A Rate Equation for Recovery, Precipitation, Transient Creep and Sintering
Materials Science and Technology (s)

A. Turos, S. Fritz, Hj. Matzke
Defects in Ion Implanted Uranium Nitride
J. Appl. Phys. (s)

T. Gouder, C. Colmenares, J.R. Naegele, J. Verbist
UPS - Study of the Surface Oxidation of Uranium by UVPhotoemission Spectroscopy
Surf. Sci. (s)

S. Heathman, U. Benedict
Comparison Between Energy Dispersive and Position Sensitive Detector Methods in High Pressure X-Ray Diffraction
High Temp. - High Pressures (s)

O. Eriksson, M.S.S. Brooks, B. Johansson
Calculated Cohesive Properties of Lanthanide and Rare-Earth-Like Actinide Elements
J. Less-Common Met. (s)

O. Eriksson, M.S.S. Brooks, B. Johansson
Theoretical Aspects of the Magnetism in the Ferromagnetic $AnFe_2$ Systems (An = U,Np,Pu and Am)
Phys. Rev. B (s)

O. Eriksson, B. Johansson, M.S.S. Brooks
Theory of Orbital Splittings Applied to $NpAl_2$
Phys. Rev. B (s)

O. Eriksson, B. Johansson, M.S.S. Brooks, H.L. Skriver
Electronic Structure of the Actinide-Rh_3 Systems and the 5f Localization in UPd_3
Phys. Rev. B 40, (1989) 9508-9518

O. Eriksson, B. Johansson, M.S.S. Brooks
Orbital Magnetism in the Itinerant Ferromagnet $NpOs_2$
Phys. Rev. B (s)

O. Eriksson, B. Johansson, M.S.S. Brooks, H.L. Skriver
Electronic Structure and Magnetic Properties of some Lanthanide and Actinide Intermetallic Laves Phase Alloys
Phys. Rev. B 40, (1989) 9519-9528

J. Fuger, R.G. Haire, W.R. Wilmarth, J.R. Peterson
Molar Enthalpy of Formation of Californium Tribromide
J. Less-Common Met. (s)

B. Lebech, M. Wulff, G.H. Lander, J. Rebizant, J.C. Spirlet, A. Delapalme
Neutron Diffraction Studies of the Crystalline and Magnetic Properties of UFe_2
J. Phys. C (s)

S. Dabos-Seignon, U. Benedict, S. Heathman, J.C. Spirlet,M. Pagès
Phase Transformation of AnX Compounds Under High Pressure:An = Np, Pu; X = Sb, Te
J. Less-Common Met. (s)

R. Jansson, K. Lassmann, A. Massih
Comparison Between the Fuel-to-Cladding Gap Conductance Models URGAP and GTEMP with Out-of-Pile Experiments
Nucl. Eng. Des. (s)

Hj. Matzke
Point Defects and Transport Properties in Carbides and Nitrides in: Selected Topics in High Temperature Chemistry - Defect Chemistry of Solids, Studies in Inorganic Chem. Vol. 9
Ed. O. Johannesen and A.G. Andersen, Elesevier (1989) 353-384

S. Bettonville, J. Goffart, J. Fuger
Organo-f-Element Thermochemistry. Actinide-Ligand Bond Disruption Enthalpies in Tris(indenyl)Actinide Hydrocarbyls
J. Organomet. Chem. (s)

O. Eriksson, M.S.S. Brooks, B. Johansson
Orbital Polarization in Narrow Band Systems: Application to Volume Collapses in Light Lanthanides
Phys. Rev. B (s)

J. Magill, S. Pickering, S. Fourcaudot, J.A. Gallego-Juarez, E. Riera, G. Rodriguez-Corral
Acoustic Aerosol Scavenging
J. Acoust. Soc. Am. 85 (1989) 2678-2680

G.H. Lander, P.J. Brown, J.M. Honig, J. Spalek
Structural and Magnetization Density Studies of La_2NiO_4
Phys. Rev. B 40 (1989) 4463-4471

M.R. Spirlet, J. Rebizant, S. Bettonville, J. Goffart
Structure of Tris(1-3-n-Ethylindenyl) Chlorothorium
Acta Crystallogr. (s)

L.R. Morss, J.W. Richardson, C.W. Williams, G.H. Lander, A.C. Lawson, N.M. Edelstein, G.V. Shalimoff
Powder Neutron Diffraction and Magnetic Susceptibility of $^{248}CmO_2$
J. Less-Common Met. (s)

G.H. Lander, W.G. Stirling, J.M. Rossat-Mignod, M. Hagen,O. Vogt
Magnetic Excitations in Monodomain Ferromagnetic Uranium Telluride
Phys. Rev. B (s)

M.R.Spirlet, J.Rebizant, C.Apostolidis, B.Kannelakopulos
Structure of Tris (n-5-cyclopentadienyl) bis propionitrile lanthanum III
Acta Cryst. C (s)

J.Rebizant, M.R.Spirlet, S.Bettonville, J.Goffart
Structure of bis (1-5-n-indenyl) uranium (IV) bis (Tetrahydroborate)
Acta Cryst. C. (s)

T.Gouder, C.A.Colmenares, J.R.Naegele, J.Verbist
UPS Photoemission Study of the C_2H_4 absorption on Uranium
J.Catalysis (s)

S.Dabos-Seignon, U.Benedict
High-Pressure Study of Np and Pu Compounds
High Pressure Research (s)

J.Staun Olsen, S.Steenstrup, L.Gerward, U.Benedict, J.Akella, G.Smith
X-Ray Diffraction Studies on Sm up to 1 Mbar
High Pressure Research (s)

L.Gerward, J.Staun Olsen, U.Benedict, H.Luo, F.Hulliger
A High-Pressure Study of Th_3P_4 and some U_3X_4 Compounds
High Pressure Research (s)

M.Wulff, O.Eriksson, B.Johansson, B.Lebech, M.S.S.Brooks, G.H.Lander, J.Rebizant, J.C.Spirlet, P.J.Brown
Experiment and Theory of Actinide Intermetallic Magnetism: A Test Case of $NpCo_2$ Europhysics Letters (s)

S.Kern, C.K.Loong, G.L.Goodman, B.Cort, G.H.Lander
Crystal Field Spectroscopy of PuO_2: Further Complications in Actinide Dioxides
J.Phys.Condens.Matter Letter (s)

J. Fuger, G.H. Lander
Die Geheimnisse der Aktiniden - Im Reich der schweren Atome
Bild Wiss. 12 (1989) 84-92

G.H. Lander, J. Fuger
Gli attinidi e le loro insolite proprietà
Scienza & Technica 89/90 (1989) 103-111

L. Gerward, J. Staun Olsen, U. Benedict, S. Dabos-Seignon
The Transformation B1 to B2 in Actinide Compounds
J. Appl. Crystallogr. (s)

T. Gouder, C.A. Colmenares, J.R. Naegele, J. Verbist
Photoemission Study of the C_2H_4 Adsorption on Uranium
J. Catal. (s)

M. Gardani, C. Ronchi
Transport and Release of Radioactive Fission Products in Nuclear Fuels: The New Analytical Method of the Code "MITRA"
Nucl. Sci. Eng. (s)

M. Wulff, O. Eriksson, B. Johansson, B. Lebech, M.S.S. Brooks, G.H. Lander, J. Rebizant, J.C. Spirlet, P.J. Brown,
Experiment and theory of actinide intermetallic magnetism:A test case of $NpCo_2$
Europhysics Letters (s)

J.-P. Glatz, H. Bokelund, S. Zierfuß
Analysis of the Off-Gas from Dissolution of Nuclear Oxide -Radiochim. Acta (s)

J.Rebizant, M.R.Spirlet, S.Betonville, J.Goffart
Structure og bis((1,2,3,3a,7a,-n)-indenyl)bis(tetrahydroborato)uraniumIV
Acta Crystallogr. C 45 (1989) 1509-1511

C.T.Walker, K.Lassmann, C.Ronchi, M.Coquerelle, M.Mogensen
The D-COM Blind Problem on Fission Gas Release: The Prediction of the TRANSURANUS and FUTURE Codes
Nucl. Eng. Des. 117 (1989) 211-233

2. Contributions to Conferences

M.S.S. Brooks, O. Eriksson, B. Johansson
Studies of Spin an Orbital Magnetism in Bands
Energy Workshop, 4.1.-6.1.1989 Trieste (Italy)

L. Gerward, J. Staun Olsen, U. Benedict
Energy Dispersive Diffraction under High Pressure: On the B1-B2 transition in Actinide Compounds
Diskussionstagung der Arbeitsgemeinschaft Kristallographie
1.3.-3.3.1989 Hannover (FRG)
Z. für Kristallographie

Hj. Matzke
Diffusion in Carbides and Nitrides
"Diffusion in Materials"
NATO Advanced Study Institute 12.3.-25.3.1989 Aussois (France)
Diffusion in Materials, Ed. A.L. Laskar and G. Brebec

Hj. Matzke
Atomic Mechanisms of Mass Transport in Ceramic Nuclear Fuel Materials
Symposium on Atomic Mechanisms of Mass Transport in Solids
29.3.-31.3.1989 Oxford (UK)
Proceedings Faraday Transactions, Special Issue

G. Grübel, D. Gibbs, J.D. Axe, G.H. Lander,H.G. Smith
High-Resolution X-Ray Scattering Study of the CDW in α-U
Meeting of the American Physical Society
20.3.-24.3.1989 St. Louis (USA)

M.S.S. Brooks, O. Eriksson, L. Nordström, B. Johansson
The Sign of the Conduction Electron Polarization in Metals and Compounds
9th General Conference of the Condensed Matter Divisionof the European Physical Society
6.3.-9.3.1989 Nice (France)

L. Nordström, O. Eriksson, B. Johansson, M.S.S. Brooks
Itinerant 4f Magnetism in $CeCo_5$
9th General Conference of the Condensed Matter Divisionof the European Physical Society
6.3.-9.3.1989 Nice (France)

19mes Journées des Actinides
29.3.-31.3.1989 Madonna di Campiglio (Italy)

J. Goudiakas, J. Fuger
Thermodynamics of some Neptunium Complex Oxides Enthalpy of Formation of α-Na_2NpO_4, β-Na_2NpO_4, β-Na_4NpO_5,K_2NpO_4, and $CaNpO_4$

S. Bettonville, J. Goffart, J. Fuger
Organo f-Element Thermochemistry
Thorium- and Uranium-Ligand Bond Disruption Enthalpies in Tris(indenyl)actinide Hydrocarbyls

S. Dabos-Seignon, U. Benedict, J.C. Spirlet, M. Pagès
High-Pressure Study of Plutonium Monoarsenide

K. Mayer, C. Apostolidis, M. Ougier
Spectroscopic Investigation of Tri- and Tetravalent Solid Americium Compounds

Ph. Raison, P. Schweiss, A. Delapalme, M.R. Spirlet, B. Kanellakopulos
Observation of Phase Transitions in Tris (Cyclopentadienyl) Chlorouranium (IV), $(C_5H_5)_3UCl$

J.P. Sanchez, K. Tomala, J. Rebizant, J.C. Spirlet,O. Vogt,
Electronic and Magnetic Properties of the $NpSb_{1-x}Te_x$ Solid Solutions from Mössbauer Spectroscopy

C. Apostolidis, J. Rebizant, M. Ougier, R. Maier, B. Kanellakopulos
Cp_3ThNCs: Preparation and Interaction with Aliphatic Nitriles and Cyclohexylisonitrile

J.R. Naegele, F. Schiavo, J.C. Spirlet,
Photoemission Study (XPS, UPS) of the Electronic Structure of PuSe

K. Zikou, T. Almeida, W. Bartscher, J.R. Naegele, J.C. Spirlet
Ethane Hydrogenolysis Studies on UNi_x and UO_2/Ni catalysts

J. Rebizant, C. Apostolidis, M.R. Spirlet, B. Kanellakopulos
The Crystal Structure Analysis of $[(U(C_5H_5)(CH_3CO_2]_4O_2$: A Tetrameric Cyclopentadenyl Acetato Complex of Uranium (IV)

G.H. Lander
New Developments in the Study of the Charge-DensityWave in Alpha Uranium

J. Rebizant, C. Apostolidis, M. Boehm, G. Hoffmann
The Crystal Structure Analysis of a New Plutonium (IV) Nitrate Hydrate: $(Pu(OH)(NO_3)_3(H_2O)_2)_2.5H_2O$
S. Kern, C.K. Loong, G.L. Goodman, B. Cort, G.H. Lander
Crystal-field Spectroscopy of PuO_2 with Pulsed Neutrons

M.R. Spirlet, J. Rebizant, S. Bettonville, J. Goffart
Comparative Structural Study of Two Novel Indenyl Complexes of Thorium

S. Bertram, G. Kaindl, J. Jove, M. Pagès, J. Gal, O. Vogt, J. Rebizant, J.C. Spirlet
Electronic Structure of Actinide Compounds from LIII-XANES Studies

E. Pleska, J.M. Fournier, J. Chiapusio, J. Rossat-Mignod, J. Rebizant, J.C. Spirlet, O. Vogt
Electrical Resistivity of the $Pu_{1-x}Y_xSb$ Solid Solution

S. Zwirner, J. Moser, U. Potzel, W. Potzel, F.J. Litterst, G.M. Kalvius, J. Gal, J.C. Spirlet
Magnetic Behaviour of $NpSn_3$ Under High Pressure

R. Maier, B. Kanellakopulos, C. Apostolidis, J. Rebizant, M.R. Spirlet
Detailed Studies of the Charge Distribution in ActinideOrganometallics with Different Site Symmetry of the Central Ion

K. Mattenberger, O. Vogt, J. Rebizant, J.C. Spirlet
Magnetic Properties of $NpSb_{0.95}Te_{0.05}$ Single Crystals

B. Kanellakopulos, K. Mayer, J. Brand, B. Powietzka
On The Magnetic Behaviour of the Americium Ion in AmO_2, Am_2O_3, $SrAmO_3$, $BaAmO_3$ and in the Oxidic Superconductive Materials $La_{2-x}Sr_xCuO_4$ and $LaBa_2CuO_{7-x}$

J.C. Spirlet, F. Wastin, C. Rijkeboer, J. Rebizant
Advance in the Preparation Chemistry of Transuranium Elements

91. Annual Meeting American Ceramic Society 23.4.-27.4.1989 Indianapolis (USA)
Proceedings Am. Ceramic Society Meeting

R.A. Verrall, Hj. Matzke, I.L. Hastings, D.H. Rose
Gas Release from SIMFUEL: Simulated High Burn-up Nuclear Fuel

P.G. Lucuta, B.J. Palmer, Hj. Matzke, D.S. Hartwig
Preparation and Characterization of SIMFUEL: Simulated High Burn-up Nuclear Fuel

A.G. Solomah, Hj. Matzke
Characterization of Leached Surfaces of Synroc Crystalline Waste Forms

H. Blank
Kinetics of Solid State Reactions and Densification in Intermediate Stage Sintering

H. Blank, K. Richter
Dihedral Angles in Cubic Carbides and Nitrides

K. Richter, H. Blank
Fabrication and Characterization of Porous Carbides and Nitrides

*

J. van Geel, H.E. Schmidt, J. Fuger
25 Years of Actinide Research at the European Institute for Transuranium Elements
ANS Meeting "Fifty Years with Nuclear Fission"
26.4.-28.4.1989 Gaithersburg, MD (USA)

L. Koch, M. Blumhofer, B. Brandalise, M. de Rossi, R. Wellum, D. Wojnowski
Conceptual Design of an On-site Laboratory for Nuclear Material Safeguards
11th Symposium on Safeguards and Nuclear Material Management
30.5.-1.6.1989 Luxembourg

L. Koch
Transuranium Element Fuel Cycle in LWR - FR Symbiosis
5th Int. Conference on Emerging Nuclear Energy Systems, 3.6.-6.6.1989 Karlsruhe (FRG)
Proceedings 5th Int. Conf. on Emerging Nuclear Energy Systems

O. Cromboom, B. Giovannone, H. Kutter, L. Koch
Application of the Radiometer Titralab System to the Measurement of Plutonium and Uranium
2nd International Conference on Analytical Chemistry in Nuclear Technology
5.6.-9.6 1989 Karlsruhe (FRG)

R. De Meester, S. Franzini, C. Szöcs, L. Koch
Determination of ^{237}Np by ICP-MS
2nd Karlsruhe Int. Conf. on Analytical Chemistry in Nuclear Technology
5.6.-9.6.1989 Karlsruhe (FRG)

B. Brandalise, M. Blumhofer, M. De Rossi, L. Koch
Robotised Isotope Analysis
2nd International Conference on Analytical Chemistry in Nuclear Technology
5.6.-9.6 1989 Karlsruhe (FRG)

Hj. Matzke, G. Della Mea, F.L. Freire Jr., V. Rigato
Determination of Hydrogen in Leached UO_2 and Synroc
Ion Beam Analysis Conference
26.6.-30.6.1989 Kingston, Ontario (Canada)
Proceedings Nucl. Instrum. Methods B

Hj. Matzke, G. Della Mea, J.C. Dran, G. Linker, B. Tiveron
Radiation Damage in Nuclear Waste Glasses Following Ion Implantation at Different Temperatures
Radiation Effects in Insulators REI-89
June 1989 Hamilton (Canada)
Proceedings Nucl. Instrum. Methods B

Hj. Matzke, A. Turos
A Channeling Study of Ion Implantation Damage in UO_2 and UN
Radiation Effects in Insulators REI-89
June 1989 Hamilton (Canada)
Proceedings Nucl. Instrum. Methods B

J. Magill
Acoustic Aerosol Scavenging
Ultrasonics International 89
3.7.-7.7.1989 Madrid (Spain)
Ultrasonics International 89 Conference Proceedings

J. Goudiakas, J. Fuger
Enthalpy of Formation of Some Neptunium (VI) Complex Oxides
44th Annual Calorimetry Conference
30.7.-4.8.1989 Oak Ridge, TN (USA)
Proceedings of Abstracts & Reports No. 95 p. 129

J.R. Naegele, F. Schiavo, J.C. Spirlet
Localization of 5f-Electrons in PuSe: A Photoemission Study (HRUPS/XPS)
9th Int. Conf. on Vacuum Ultraviolet Radiation Physics
17.7.-21.7.1989 Honolulu, Hawaii (USA)
Proceedings Physica Scripta

J.R. Naegele, L. Havela, V. Sechovsky
Determination of Band Electron Character in UMn_2 by Energy Dependent Photoelectron Spectroscopy
4th Int. Conf. on Electron Spectroscopy (ICES4)
10.7.-14.7.1989 Honolulu, Hawaii (USA)
Proceedings J. Electr. Spect. Rel. Phen.

S. Dabos-Seignon, U. Benedict
High-Pressure Study of Neptunium and Plutonium Compounds
International High-Pressure Conference of AIRAPT and EHPRG
17.7.-21.7.1989 Paderborn (BRD)
Proceedings High-Pressure Research

J. Staun Olsen, S. Steenstrup, L. Gerward, U. Benedict,
J. Akella, G. Smith
X-Ray Diffraction Studies on Samarium up to one Megabar Pressure
International High-Pressure Conference of AIRAPT and EHPRG
17.7.-21.7.1989 Paderborn (BRD)
Proceedings High-Pressure Research

J.-F. Babelot, J.C. Closset, J.-P. Glatz, T. Huber
J.A. Gallego-Juarez, E. De Sarabia, G. Rodriguez-Corral
Absorption of a Toxic Gas on Aerosol Particles: Influence of an Acoustic Field
Ultrasonics International 89
3.7.-7.7.1989 Madrid (Spain)

S. Pickering, J. Magill, S. Fourcaudot, J.A. Gallego-Juarez, E. De Sarabia, G. Rodriguez-Corral
Ultrasonic Aerosol Agglomeration
Ultrasonics International 89
3.7.-7.7.1989 Madrid (Spain)

L. Gerward, J. Staun Olsen, U. Benedict, H. Luo
F. Hulliger
A High-Pressure Study of Th_3P_4 and Some U_3X_4 Compounds
Int. Conf. on High Pressure Science and Technology
17.7.-21.7.1989 Paderborn (FRG)

3rd Workshop on Actinides under Pressure
24.-25.7.1989, Karlsruhe, FRG
Proc. in High Pressure Res. (1990)

S.Dabos-Seignon, E.Gering, U.Benedict, J.C.Spirlet, M.Pagès
High-Pressure X-Ray Diffraction Study of the δ-Phase in the Uranium-Neptunium Binary System

M.S.S.Brooks, O.Eriksson, B.Johansson
The Relativistic Equation of State of Actinide Metals and Compounds

R.G.Haire, S.Heathman, U.Benedict
A Structural Study of Promethium Metal under Pressure

J.Staun Olsen, L.Gerward, U.Benedict, S.Dabos-Seignon, J.P.Itié
High-Pressure Phases of Thorium and Uranium Compoundswith the Rocksalt Structure

E.Gerin, J.P.Dancausse, L.Gerward, J.Staun Olsen, O.Vogt
High-Pressure Phase Transitions in U(P,S)

M.Gensini, E.Gering, S.Heathman, J.C.Spirlet
High-Pressure Phases of Plutonium Monoselenide studied by X-Ray Diffraction

J.P.Dancausse, E.Gering, S.Heathman
Pressure-Induced Phase Transition in ThO_2 and PuO_2

J.C.Spirlet, E.Bednarczyk, J.Kalbusch, A.Moens, J.Rebizant, C.Rijkeboer, F.Wastin
Availability and Sample Preparation of Actinide Compounds

*

G. Van Goethem, K. Lassmann, H. Wider
Status of the European Accident Code EAC-2 for LMFBR Safety Analysis with Emphasis on the MOL7C/7 Pretest Calculations
10th Int. Conf. on Structural Mechanics in Reactor Technology (SMIRT)
14.8.-18.8.1989 Anaheim, California (USA)

P. Bottomley, M. Coquerelle
Microstructure and Elemental Analysis of Samples from a Melted-Down Core of a Reactor (TMI-2)
12th Int. Congress on X-Ray Optics and Microanalysis
28.8.-1.9.1989 Cracow (Poland)

Hj. Matzke
Mass Transport in Carbides and Nitrides
NATO Advanced Research Workshop "The Physics and Chemistry of Carbides, Nitrides and Borides"
18.9.-22.9.1989 Manchester (UK)

S. Pickering
The Resuspension of Radioactive Dusts in Fires
European Aerosol Conference
18.9.-23.9.1989 Wien (Austria)

Actinides-89
24.9.-29.9.1989 Tashkent (USSR)

J. Fuger
Chemical Thermodynamics of the Actinides and Their Compounds: An Overview of Recent Advances

G.H. Lander, W.G. Stirling, J. Rossat-Mignod, S. Kern,C.K. Loong
Neutron Inelastic Scattering Studies of Actinide Systems

U. Benedict, S. Dabos-Seignon, L. Gerward, J.P. Itié H. Luo, J. Staun Olsen
Combined XRD, Optical Reflectivity, and X-Ray Absorption Study of Actinide Pnictides and Chalcogenides: A Triple Way of Approaching 5f Behaviour Under Pressure

S. Dabos-Seignon, U. Benedict, J.C. Spirlet, M. Pagès
Compression Studies up to 55 GPa on NaCl Type Compounds AnX: An = Np, Pu and X = Sb, Te

J.R. Naegele
Electronic Structure Investigation of Actinides by Photoelectron Spectroscopy

B. Johansson, O. Eriksosn, M.S.S. Brooks
Metals and Intermetallic Compounds, Electronic Structureand Magnetic Properties

International Conference on the Physics of Highly Correlated Electron Systems, September 1989, Santa Fe, NM, USA

G.H.Lander
Neutron Scattering Studies of Actinide Compounds: Evidence for Hybridization Effects

K.Mattenberger, O.Vogt, J.Rebizant, J.C.Spirlet, J.Rossat-Mignod, P.Bultet, E.Pleska
Magnetic Properties of NpSb-NpTe Mixed Single Crystals

G.M.Kalvius, S.Zwirner, U.Potzel, J.Moser, W.Potzel, F.J.Litterst, J.Gal, J.C.Spirlet
High-Pressure Investigation of $NpSn_3$

J.M.Fournier, E.Pleska, J.Rossat-Mignod, J.Rebizant, J.C.Spirlet, O.Vogt
Electrical Resistivity of Plutonium Monochalcogenides

Symposium on "Transuranium Elements Today and Tomorrow"
26.-27.10.1989, Karlsruhe, FRG
Proc. in J.Nucl.Mat. 166 (1989)

M.Boge, D.Bonnisseau, P.Burlet, J.M.Fournier, E.Pleska,S.Quezel, J.Rebizant, J.Rossat-Mignod, J.C.Spirlet, M.Wulff
Magnetic and Electrical Properties of $NpRu_2Si_2$
p.77-82

U.Benedict, S.Dabos-Seignon, C.Dufour, H.Luo, S.Heathman
Transuranium Materials under extreme Pressures
p.48-55

J.C.Spirlet
New Techniques in the Preparative Chemistry of Transuranium Materials
p.41-47

J.R.Naegele
Surface Analysis of Actinide Materials
p.59-67

*

M. Coquerelle, Hj. Matzke
MOX-fuel Studies at the European Institute for Transuranium Elements
IAEA Technical Committee Meeting on Recycling of Plutonium and Uranium in Water Reactor Fuels
13.11.-16.11.1989 Cadarache (France)

A.M. Bevilacqua, Hj. Matzke
Comparacion de Valores de KIC en Residuos Nucleares
Vitrificados Obtenidos Mediante Indentaciones Vickers y Fractometria "Short Rod"
Meeting Asociacion argentina de tecnologia nuclear 4.12-7.12.1989 Bariloche (Argentina)

3. Reports and Technical Notes

H.E.Schmidt, J.Richter, L.Ruczka, R.Wellum (Eds)
Annual Report 1988
EUR 12385 EN (1989)

H.A. Tasman
Fast Positioning and Data Acquisition Device for Profile Recording
EUR 12300 EN (1989)

M. Gardani, C. Ronchi
"MITRA" An Advanced Code to Calculate Radionuclide Release from Nuclear Fuels Under General Irradiation Conditions
EUR 12375 EN (1989)

R.O.A. Hall, A.J. Jeffery, M.J. Mortimer, J.C. Spirlet
Heat Capacity of PuAs Between 10 and 300 K
AERE-R-13476 (1989)

R.O.A. Hall, A.J. Jeffery, M.J. Mortimer, J.C. Spirlet
Heat Capacity of PuTe Between 10 and 300 K
AERE-R-13490 (1989)

P.G. Lucuta, B.J. Palmer, Hj. Matzke, D.S. Hartwig
Preparation and Characterization of SIMFUEL: Simulated Candu High-Burnup Nuclear Fuel
AECL Report, Chalk River, Ontario, Canada

M. Gardani, J. van de Laar
Program FUTURE Fuel Transient Ultimate Response
User's Guide - Version 0.4
K 0289115 (1989)

M. Gardani, J. van de Laar
Program TEMPGAP Temperature Profile and Gap Conductance
User's Guide - Version 0.5
K 0289116 (1989)

M. Gardani, C. Ronchi
Program MITRA Multicomponent Isotope TRAnsport
User's guide - Version 1.0
K 0289117 (1989)

M. Gardani
Program FORMALISM Draft for an Internal Programming Standard - Version 1.5
K 0289118 (1989)

G.J. Small
An Assessment of the "Future" Model against Recent Experimental Data
K 0289119 (1989)

K. Lassmann
Analyse eines DWR Brennstabs mit dem TRANSURANUS Rechenprogramm
K 0289120 (1989)

G.J. Small
A Simplified Approach to Fission Gas Release Modelling (Based on the Code "FUTURE")
K 0289121 (1989)

K. Lassmann, J. van de Laar
Transuranus - Änderungsprotokoll Version 1, Modifikation 2, Jahr 1989 ('V1M2J89')
K 0289122 (1989)

P.E. Potter
The Behaviour of Fission Products in Irradiated LWR Fuels, An Introduction to their Chemical Behaviour
K 0289123 (1989)

K. Lassmann, L.A. Nordström, J. van de Laar
Analyse von SWR Brennstäben mit dem TRANSURANUS Rechenprogramm
K 0289124 (1989)

H.A.Tasman,
Differential Pyrometry in the Infrared, Part I - Optics
K 0289125 (1989)

C.Ronchi, F.Turrini
Thermochemical Data for Reactor Materials
K 0289126 (1989)

J.-F. Gueugnon, K. Richter
Standards U et $(U,Pu)O_2$ pour spectromètre à rayons X
K 0289127 (1989)

Annex B: Organisational Chart

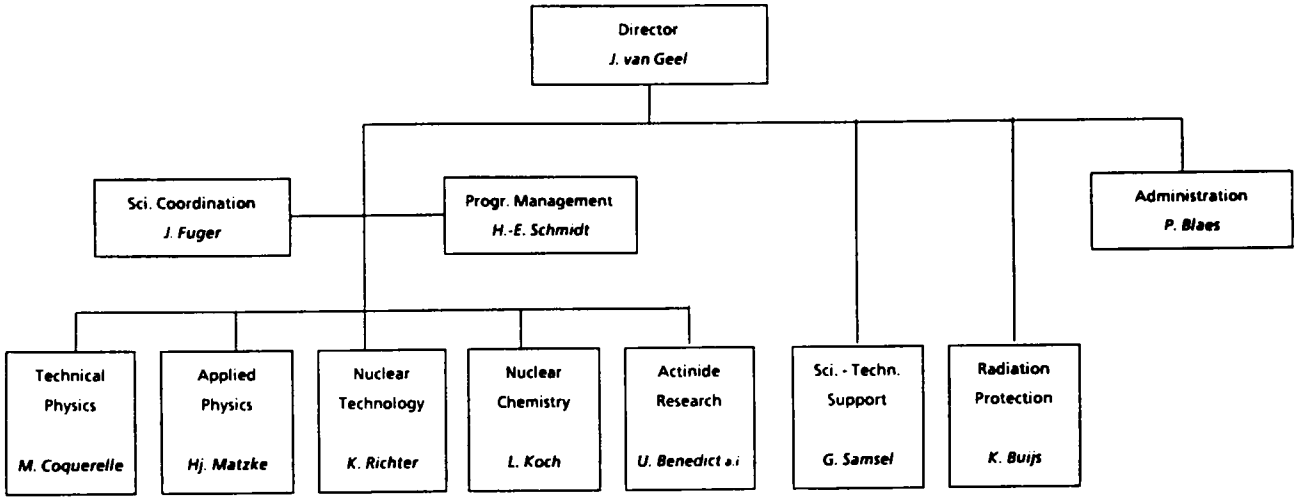

Annex C: List of Tables and Figures

1. Figures

2. Tables

Annex D: Glossary of Acronyms and Abbreviations

AERE: Atomic Energy Research Establishment
BOL.: Beginning of Life (of a fuel pin)
BUMMEL: Irradiation experiment for bubble mobility measurements at HFR
CBNM: Central Bureau for Nuclear Measurements, Geel
CEA: Commissariat à l'Energie Atomique
CEN: Centre d'Etudes Nucléaires
CNRS: Centre National de la Recherche Scientifique
DARM: Destructive Analysis of Reference Materials
DCS: Direction Contrôle de Sécurité (DGXII/F), Luxembourg
EAC: European Accident Code
ECN: Energie Centrum Nederland
EDAX: Energy-Dispersive X-Ray Analysis
EFR: European Fast Reactor
EMPA: Electron Microprobe Analysis (also EPMA)
ENEA: Entente Nazionale dell' Energia Alternativa
ERDA: Elastic Recoil Detection Analysis
ESTER: Hot vitrification pilot plant (Ispra)
ETH: Eidgenössische Technische Hochschule (Zürich)
FBR: Fast Breeder Reactor
FUTURE: Code for fuel transient calculations
GSP: Gel-Supported Precipitation
HAW: Highly Active Waste
HF: High Frequency
HPUPS: High Performance Ultraviolet light induced Photoelectron Spectroscopy
HPXRD: High-Pressure X-Ray Diffraction
HRUPS: High-resolution ultraviolet photoemission spectroscopy
IAEA: International Atomic Energy Agency (Vienna)
ICP-MS: Inductively Coupled Plasma Mass Spectrometry
ICP-OES: Inductively Coupled Plasma Optical Emission Spectroscopy
ILLW: Intermediate Level Liquid Waste
ITU: Institute for Transuranium Elements
JRC: Joint Research Centre
KNK. Kompakte Natrium-gekühlte Kernenergieanlage Karlsruhe
KORIGEN: Depletion code
LMFBR: Liquid Metal (cooled) Fast Breeder Reactor
LWR: Light Water Reactor
MA: Minor Actinides (Np, Am, Cm)

MITRA: Code to calculate the release of radio nuclides
MOX: Mixed Oxide fuel
NILOC: Nitride Irradiation with Low Carbon Content
NIMPHE: Nitride Irradiation in the PHENIX reactor
OECD: Organisation for Economic Cooperation and Development
OXAL: Oxalate Precipitation Process
PFR: Prototype Fast Reactor
PHEBUS: French test reactor, Cadarache
PHENIX: French prototype fast reactor
PIE: Post Irradiation Examination
PMMA: Polymethacrylate (Plexiglass)
PUREX: Plutonium and Uranium Recovery by Extraction
PVC: Polyvinylchloride
PWR: Pressurized Water Reactor
REPRO: Sub-Project "Reprocessing of Nuclear Fuels"
SIMFUEL: Th-based fuel with major non-volatile fission products (simulated)
SEM: Scanning Electron Microscopy
SNR-300: German prototype fast reactor
SUPERFACT: Minor Actinide Irradiation in Phenix
SUPERPHENIX: French fast reactor
TEM: Transmission Electron Microscopy
TIG: Tungsten Inert Gas Welding
TRANSURANUS: Fuel behaviour code
TUAR: TU Annual Report
XRF: X-Ray Fluorescence

Previous Progress Reports of the Institute for Transuranium Elements

TUSR	Period	COM-Nr	EUR-Nr
1	Jan - Jun 1966	1580	
2	Jul - Dec 1966	1522	
3	Jan - Jun 1967	1745	
4	Jul - Dec 1967	2007	
5	Jan - Jun 1968	2172	
6	Jul - Dec 1968	2300	
7	Jan - Jun 1969	2434	
8	Jul - Dec 1969	2576	
9	Jan - Jun 1970	2664	
10	Jul - Dec 1970	2750	
11	Jan - Jun 1971	2833	
12	Jul - Dec 1971	2874	
13	Jan - Jun 1972	2939	
14	Jul - Dec 1972	3014	
15	Jan - Jun 1973	3050	
16	Jul - Dec 1973	3115	
17	Jan - Jun 1974	3161	
18	Jul - Dec 1974	3204	
19	Jan - Jun 1975	3241	
20	Jul - Dec 1975	3289	
21	Jan - Jun 1976	3358	
22	Jul - Dec 1976	3384	
23	Jan - Jun 1977	3438	6475 E
24	Jul - Dec 1977	3484	7209 E
25	Jan - Jun 1978	3526	7459 E
26	Jul - Dec 1978	3582	7227 E
27	Jan - Jun 1979	3657	7483 E
28	Jul - Dec 1979	3714	7509 E
29	Jan - Jun 1980	3822	7857 E
30	Jul - Dec 1980	3846	8230 E
31	Jan - Jun 1981	3898	8447 E
32	Jul - Dec 1981	3927	8777 E
33	Jan - Jun 1982	3990	9581 E
34	Jul - Dec 1982	4048	10251 E
35	Jan - Jun 1983	4094	10266 E
36	Jul - Dec 1983	4117	10454 E
37	Jan - Jun 1984	4150	10470 E
38	Jul - Dec 1984	4165	11013 E
39	Jan - Jun 1985	4201	11835 E
40	Jul - Dec 1985	4263	11836 E
TUAR			
86	Jan - Dec 1986	4302	12233 E
87	Jan - Dec 1987	------	11783 E
88	Jan - Dec 1988	------	12385 E
89	Jan - Dec 1989		12849 E

Previous Programme Progress Reports were confidential for a period of two years. Since 1977 they are made freely accessible after that period as EUR-Reports. They can be ordered from the Office for Official Publications of the European Communities, 2 rue Mercier, L-2985 Luxemburg, Tel. 49 92 81, Telex PUBOF LU 1324 b

This report was compiled and edited by H.E. Schmidt, J. Richter, and L. Ruczka.

Inquiries for more details should be adressed to the Programme Office, Institute for Transuranium Elements, P.O. Box 2340, D-7500 Karlsruhe, Phone 07247-84386, FAX 07247-4046

For further information concerning JRC programmes please contact the Directorate General Science, Research and Development of the Commission of the European Communities, 200 rue de la Loi, B-1049 Brussels, Belgium.